

1 **Provenance of exhalites associated with the Lemarchant volcanogenic massive**  
2 **sulphide (VMS) deposit, central Newfoundland, Canada: Insights from Nd isotopes**  
3 **and lithogeochemistry**

4

5 Stefanie Lode<sup>1\*</sup>, Stephen J. Piercey<sup>1</sup>, Jonathan Cloutier<sup>2</sup>

6

7 <sup>1</sup>*Department of Earth Sciences, Memorial University, 300 Prince Philip Drive, St.*

8 *John's, NL, Canada, A1B 3X5*

9 <sup>2</sup>*Department of Earth Sciences, University of St. Andrews, St. Andrews, Scotland, UK,*

10 *KY16 9AL*

11 *\*Correspondence (slode@mun.ca)*

12

13

14

15 **Abstract:** Neodymium isotope data on exhalites and tuffs from the Cambrian  
16 Lemarchant volcanogenic massive sulphide (VMS) deposit provide insights into the  
17 tectonic environment of the Tally Pond group, Canada. New data from exhalites from the  
18 Lemarchant area show evolved values of  $\epsilon\text{Nd}_{513} = -6.0$  to  $-1.8$ , whereas the associated  
19 volcanic rocks have  $\epsilon\text{Nd}_{513}$  of  $+0.4$  to  $+1.4$ . The Lemarchant exhalite  $\epsilon\text{Nd}$  compositions  
20 overlap the underlying Ganderian Neoproterozoic Sandy Brook Group ( $\epsilon\text{Nd}_t = -6.5$  to  
21  $-1.9$ ) and Crippleback Intrusive Suite ( $\epsilon\text{Nd}_t = -5.9$  to  $-5.2$ ). The evolved Nd isotopic  
22 signatures suggest that the volcanic rocks of the Tally Pond group were formed upon  
23 Ganderian arc basement, which itself was possibly built upon, or proximal to, the

24 Gondwanan Amazonian margin. Erosion of older crustal material and Tally Pond group  
25 volcanic rocks, together with coeval eruption of the volcanic rocks, released Nd-rich  
26 detritus into the water column. Uptake of eroded detrital and scavenged Nd resulted in  
27 mixed Nd sources (juvenile and evolved), which are archived in the exhalites. The results  
28 of this study are of significance not only for occurrences of exhalites within the Tally  
29 Pond group, but also have exploration implications for VMS districts globally.

30

31

32

33 The Tally Pond group, central Newfoundland Appalachians, Canada, represents a  
34 volcanic belt that hosts abundant volcanogenic massive sulphide (VMS) deposits that are  
35 locally genetically associated with exhalites (Fig. 1 A-B; Franklin 1981; Lydon 1984;  
36 Swinden 1991; Squires & Moore 2004). Exhalites are metalliferous sedimentary rocks  
37 and are also described as metalliferous/hydrothermal mudstones, iron formation, tetsukiei  
38 ('iron quartz'), tuffite, vasskis ('Weißkies' = 'white sulphide', also used for sulphidic  
39 black chert; Peter & Goodfellow 1996; Spry *et al.* 2000; Peter 2003; Hannington 2014).

40 Exhalites represent a hiatus in the volcanic activity where the deposition of hydrothermal  
41 products is dominant over the abiogenic background sedimentation and/or deposition of  
42 volcanoclastic-epiclastic material (Lydon 1984). The lithogeochemical signatures of  
43 exhalites can be utilized to discriminate between predominantly hydrothermally or  
44 detritally (i.e., non-hydrothermal) derived material in exhalative rocks (Fig. 2A; Boström  
45 *et al.* 1972; Boström 1973; Peter 2003; Lode *et al.* 2016). The Lemarchant exhalites are  
46 dominated by elevated Fe/Al and Zn-Pb-Cu contents compared to detrital sedimentary

47 rocks, and have shale-normalized negative Ce and positive Eu anomalies, indicative of  
48 deposition from high temperature (>250°C) hydrothermal fluids within an oxygenated  
49 water column, rather than being the product of predominantly detrital sedimentation (Fig.  
50 2A-B; Boström & Petersen 1969; Boström *et al.* 1972; Boström 1973; Sverjensky 1984;  
51 de Baar *et al.* 1988; German & Von Damm 2003; Peter 2003; Lode *et al.* 2015).

52

53 The Tally Pond group, which is part of the Dunnage Zone, Newfoundland, Canada,  
54 belongs to the Cambrian (~515 Ma) to Permian (~275 Ma) Appalachian-Caledonide  
55 mountain belt that hosts numerous VMS deposits, including the past-producing Duck  
56 Pond and Boundary mines, and the precious metal-bearing Lemarchant deposit (Fig. 1A-  
57 B; Williams 1979; Swinden 1988, 1991; Evans & Kean 2002; Grenne & Slack 2003;  
58 Rogers *et al.* 2007; van Staal & Barr 2011; Piercey *et al.* 2014; Hollis *et al.* 2015). The  
59 Tally Pond group (~513-509 Ma) volcanic rocks and related massive sulphide  
60 mineralization formed during arc rifting during the construction of the Cambrian to Early  
61 Ordovician Penobscot Arc, which is known to be built upon Ganderian Neoproterozoic  
62 (~563 Ma) arc basement of the Crippleback Intrusive Suite and the coeval Sandy Brook  
63 Group (Pollock *et al.* 2002; Zagorevski *et al.* 2007; Piercey *et al.* 2014). In the  
64 Neoproterozoic and Early Cambrian Ganderia was located north-west of the Gondwanan  
65 Amazonian margin (Fyffe *et al.* 2009; van Staal *et al.* 2012; Murphy *et al.* 2014). The  
66 Penobscot Arc represented the leading edge of Ganderia in a supra-subduction zone  
67 setting and arc rifting was initiated due to slab roll-back along this margin (Jenner &  
68 Swinden 1993; Schulz *et al.* 2008; Murphy *et al.* 2014). The basement to the Ganderian  
69 arc is not exposed; however, detrital zircon and Nd isotopic studies indicate the presence

70 of older crustal rocks that were derived from the Gondwanan Amazonian craton (Nance  
71 *et al.* 2008; Schulz *et al.* 2008). Rifting of the Penobscot Arc led to the formation of  
72 volcanogenic massive sulphide (VMS) mineralization and associated hydrothermal  
73 sedimentary rocks of the Tally Pond group (Rogers *et al.* 2006; Copeland *et al.* 2009;  
74 Zagorevski *et al.* 2010; Piercey *et al.* 2014; Lode *et al.* 2016). During rifting of the  
75 Penobscot Arc there was extension, massive sulfide formation, and the genesis of  
76 exhalites that formed from the deposition from buoyant hydrothermal plumes from black  
77 smokers (Hekinian *et al.* 1993; Hannington *et al.* 1995; German & Von Damm 2003).  
78  
79 These black smokers and associated exhalites occur where hydrothermal fluids are  
80 focused along deep synvolcanic faults in extensional settings (e.g., ocean ridges, rifted  
81 arcs, or backarc basin spreading centres; Fig. 3; Lydon 1984; Hannington *et al.* 2005;  
82 Gibson *et al.* 2007). The hydrothermal fluids consist of modified seawater, which is  
83 entrained through oceanic or rift-related continental crust, and are variably metal bearing  
84 with Fe, Mn, Cu, Pb, and Zn, as well as reduced S and Si (Von Damm 1990; German &  
85 Von Damm 2003; Galley *et al.* 2007; Tivey 2007; Huston *et al.* 2010). The metals and  
86 other ligands are generally derived from seawater and leached from host rocks (e.g.,  
87 metals, Si±S; Fig. 3; Hannington *et al.* 2005; Huston *et al.* 2011). Hydrothermal plume-  
88 derived Fe-oxyhydroxides are efficient scavengers of trace metals (e.g., oxyanions such  
89 as  $\text{HPO}_4^{2-}$ ,  $\text{HVO}_4^{2-}$ ,  $\text{CrO}_4^{2-}$ ,  $\text{HAsO}_4^{2-}$ ) and rare earth elements (REE) plus Y from  
90 seawater (Mills & Elderfield 1995; Rudnicki 1995). A rifted arc environment exposes  
91 rock units of different ages, hence varying Nd isotopic signatures, which contribute  
92 detrital material to the hydrothermal matter in the exhalative sedimentary rocks due to

93 erosional and weathering processes (Keto & Jacobson 1988; Mills & Elderfield 1995).  
94 Therefore, exhalites not only record seawater REE (including Nd) but also the diverse  
95 provenance components of the detrital sources at the time of formation, even though the  
96 detrital matter is only a minor constituent compared to the hydrothermal matter (Mills &  
97 Elderfield 1995; Peter 2003; Lode *et al.* 2015).

98

99 By using various isotopic tracers, such as Nd isotopes, it is possible to decipher the  
100 potential sources of various components in hydrothermal sedimentary rocks. The Nd  
101 isotopic system is specifically useful for understanding the relative roles of evolved  
102 versus juvenile crust, and provides further insight into the tectonic environment and  
103 provenance of the exhalites, as it is robust and not significantly modified by diagenetic,  
104 hydrothermal, and metamorphic processes (McCulloch & Wasserburg 1978; McLennan  
105 *et al.* 2003). In addition, the separation of Sm-Nd in Earth's reservoirs is particularly  
106 useful in delineating juvenile versus evolved crust and the time-integrated sources of  
107 materials in Earth materials (McCulloch & Wasserburg 1978; Rollinson 1993; McLennan  
108 *et al.* 2003). The Tally Pond group volcanic rocks have  $\epsilon\text{Nd}$  signatures that are typically  
109 positive, whereas their basement rocks, i.e., the rifted arc rocks of the Neoproterozoic  
110 Crippleback Intrusive Suite and the bimodal volcanic rocks of the Sandy Brook Group  
111 show more evolved  $\epsilon\text{Nd}$  values (McLennan *et al.* 1993; Rogers *et al.* 2006; Nance *et al.*  
112 2008; McNicoll *et al.* 2010; Piercey *et al.* 2014). Given the level of preservation of  
113 stratigraphy of the lithofacies in the Lemarchant deposit, including the exhalites, this  
114 deposit is an excellent location to understand the provenance of exhalites in ancient rifted  
115 arcs. Correspondingly, the Nd isotopic signatures in the exhalites may be useful in

116 outlining their provenance and the potential contributions of local versus basement versus  
117 distal sources in their genesis. Thus, the purpose of this study is to: 1) determine the  
118 sources of Nd in the exhalites and massive sulphides of the Lemarchant deposit; and 2)  
119 because the Tally Pond group is formed upon Ganderian and possibly older basement  
120 rocks, to evaluate the relative roles of mantle and evolved crustal inputs that contributed  
121 to the Lemarchant hydrothermal sedimentary rocks using the Nd isotope compositions of  
122 exhalites.

123

#### 124 **Regional Geology**

125 The Tally Pond group is located within the Central Mobile Belt, Newfoundland, Canada,  
126 which is part of the Cambrian (~515 Ma) to Permian (~275 Ma) Appalachian mountain  
127 belt (Williams 1979; Swinden 1988; Rogers *et al.* 2007; van Staal & Barr 2011). The  
128 Newfoundland Appalachians are divided into four tectonostratigraphical zones (from  
129 west to east): Humber, Dunnage, Gander and Avalon zones (Fig. 1A; Williams 1979;  
130 Swinden 1988, 1991). The Dunnage Zone represents the Central Mobile Belt (Williams  
131 *et al.* 1988; Swinden 1991; Rogers *et al.* 2007). These zones result from and were  
132 affected by the successive accretion of three micro-continental blocks during the Early  
133 Palaeozoic to Middle Palaeozoic (i.e., Dashwoods, Taconic orogenesis; Ganderia, Salinic  
134 orogenesis; and Avalonia, Acadian orogenesis) and related interoceanic arcs and backarcs  
135 (Swinden 1991; Zagorevski *et al.* 2010). In the Palaeozoic (Middle Cambrian to  
136 Ordovician), these ribbon-shaped micro-continental blocks separated from Gondwana  
137 and Laurentia, forming peri-Gondwanan and peri-Laurentian terranes and subsequently  
138 accreted to Laurentia creating the composite Laurentian margin (Rogers *et al.* 2007;

139 Zagorevski *et al.* 2010; van Staal & Barr 2011). The Exploits Subzone represents two  
140 phases of arc-backarc formation: the Cambrian to Early Ordovician Penobscot Arc and  
141 the Early to Middle Ordovician Victoria Arc (Zagorevski *et al.* 2010). The Tally Pond  
142 group and its VMS deposits (Duck Pond and Boundary mines; Lemarchant deposit; Fig.  
143 1B) are hosted in the lower Victoria Lake supergroup within the Exploits Subzone, which  
144 is comprised of Cambrian to Ordovician volcanic and sedimentary rocks (Dunning *et al.*  
145 1991; Rogers *et al.* 2007; McNicoll *et al.* 2010; van Staal & Barr 2011). The Victoria  
146 Lake supergroup is further subdivided into six assemblages (Zagorevski *et al.* 2010;  
147 Piercey *et al.* 2014), which are bounded by faults, and are from east to west: 1) the Tally  
148 Pond group; 2) the Long Lake group; 3) the Tulks group; 4) the Sutherlands Pond group;  
149 5) the Pats Pond group; and 6) the Wigwam Pond group; the Tulks, Long Lake, and Tally  
150 Pond groups are known to host VMS deposits. These six tectonic assemblages yield U-Pb  
151 zircon ages ranging from ~513 to 453 Ma (Dunning *et al.* 1987; Evans *et al.* 1990;  
152 Dunning *et al.* 1991; Evans & Kean 2002; Zagorevski *et al.* 2007; McNicoll *et al.* 2010).  
153 Furthermore, the Tally Pond group is informally subdivided into the felsic volcanic rock  
154 dominated Bindons Pond formation (also referred to as Boundary Brook formation;  
155 Pollock 2004) and the mafic volcanic rock dominated Lake Ambrose formation (Rogers  
156 *et al.* 2006). The latter contains island arc tholeiitic basalts to andesites with  $\epsilon\text{Nd}_{511}$  of  
157 +3.1 (Dunning *et al.* 1991; Evans & Kean 2002; Rogers *et al.* 2006), whereas the former  
158 contains predominantly transitional to calc-alkalic rhyolitic to dacitic rocks with  $\epsilon\text{Nd}_{511}$   
159 of +1.8 to +2.6 (Rogers *et al.* 2006; McNicoll *et al.* 2010; Piercey *et al.* 2014). The  
160 Cambrian felsic volcanic rocks of the Bindons Pond formation contain inherited zircons  
161 with Neoproterozoic U-Pb ages of 563 Ma (McNicoll *et al.* 2010).

162

163 **Deposit Geology and Lithofacies**

164 The Lemarchant VMS deposit is hosted within the Bindons Pond formation and is capped  
165 by a <1 to 20 m thick layer of exhalites occurring at the contact between the bimodal  
166 volcanic rocks of the Bindons Pond and Lake Ambrose formations (Fig. 4A; Copeland *et*  
167 *al.* 2009; Fraser *et al.* 2012; Lode *et al.* 2015). These sulphide-rich exhalites extend  
168 discontinuously around the massive sulphides for one to four kilometres (Copeland *et al.*  
169 2009; Fraser *et al.* 2012; Lode *et al.* 2015). Three main types of exhalatives occur at the  
170 Lemarchant deposit: 1) exhalites immediately on top of massive sulphide mineralization  
171 between the felsic and mafic volcanic rocks (exhalative-massive sulphide (EMS)-type;  
172 Fig. 4A-C, G-H); 2) exhalites extending laterally outwards from mineralization, but at the  
173 same stratigraphical level and without immediate association with mineralization (felsic-  
174 exhalative-mafic (FEM)-type; Fig. 4D); or 3) interflow exhalites within the hanging wall  
175 basaltic rocks (IFE-type; Fig. 4E). Interflow exhalites occur commonly within 15 metres  
176 above the massive sulphide mineralization, but are present up to 70 metres  
177 stratigraphically above the ore horizon. Crystal lithic vitric (locally vitric crystal) tuff is  
178 intercalated with the exhalites and surrounding mafic and felsic volcanic lithologies and  
179 commonly contains chloritized glass shards and locally euhedral apatite phenocrysts (Fig  
180 4F). Independent of their stratigraphical positions, the exhalites are brown to black,  
181 graphite-rich, finely laminated, and contain fine carbonaceous/organic-rich laminae that  
182 are intercalated with siliciclastic, volcanoclastic and/or amorphous kidney-shaped  
183 chert±apatite layers (Fig. 4A-C). The main sulphide phases are pyrite (framboidal,  
184 massive, and euhedral) and pyrrhotite, with minor marcasite, chalcopyrite, sphalerite,



185 arsenopyrite and galena (Fig. 5A-C). Sphalerite commonly displays chalcopyrite disease  
186 (Fig. 5A). Contents of chalcopyrite, sphalerite, and galena increase proximal to  
187 mineralization. The sulphides occur both parallel to bedding, and in later stage, stringer-  
188 like veins (Fig. 4A-E). Ba-mineral phases include barite ( $\text{BaSO}_4$ ; Fig. 4F), the Ba-rich  
189 feldspar celsian ( $\text{BaAl}_2\text{Si}_2\text{O}_8$ ), and a barian K-feldspar with <2wt% Ba (hyalophane or  
190 barian adularia  $(\text{K,Ba})\text{Al}(\text{Si,Al})_3\text{O}_8$ ). Barite locally forms anhedral (semi-)continuous  
191 layers or occurs as bladed crystals in vugs or veins, which are often associated with  
192 bladed Ca-Fe-Mg-Mn-carbonates.

193

194 All types of the Lemarchant exhalites (proximal, distal, and interflow) have variable  
195 contributions of hydrothermal (high Fe/Al and base metal values; Fig. 2A) and detrital  
196 components (lower Fe/Al and base metal values). Furthermore, they display positive  
197 shale normalized Eu anomalies and positive Ce anomalies (Fig. 2B). These signatures  
198 suggest precipitation from reduced, high-temperature (>250°C) hydrothermal vent fluids  
199 in an oxygenated water column in a hydrothermal vent proximal setting (Lode *et al.*  
200 2015; 2016). Deposition into an oxygenated water column in a vent proximal  
201 environment is also supported by the presence of barite in both the exhalites and  
202 associated massive sulphides, as well as the S-isotopic signatures of sulphides within the  
203 exhalites (Lode *et al.* 2017). The  $\delta^{34}\text{S}$  systematics (ranging from -38.8‰ to +14.4‰, with  
204 an average of  $\sim -12.8$ ‰) indicate that S was predominantly biogenically-derived via  
205 microbial/biogenic sulphate reduction of seawater sulphate, microbial sulphide oxidation,  
206 and microbial disproportionation of intermediate S compounds but also from inorganic  
207 thermochemical sulphate reduction (Fig. 5A-D). The latter is more pronounced in

208 sulphides from the proximal EMS-type Lemarchant exhalites (Fig. 5D; Lode *et al.* 2017).  
209 Combined detailed lithogeochemical, mineralogical, and S- and Pb-isotopic studies and  
210 the stratigraphical context of these sulphide-rich mudstones, and intimate association  
211 with massive sulphides, suggests that they are hydrothermal in origin and formed from  
212 black smoker plume fallout and true exhalites rather than detrital sedimentary rocks  
213 (Lode *et al.* 2015; 2016; 2017).

214

## 215 **Methodology**

### 216 *Sampling, methods, and quality control and quality assurance (QA/QC)*

217 Samples were collected during stratigraphical mapping and drill core logging of the  
218 Lemarchant deposit from drill holes that have exhalites and include the Lemarchant Main  
219 Zone, the Northwest and 24 zones, as well as the North and South targets (Fig. 6A).  
220 Samples were taken from representative exhalite types (EMS, FEM, and IFE), tuff, and  
221 surrounding mafic and felsic volcanic units. The whole rock lithogeochemical data were  
222 previously evaluated and presented in Lode *et al.* (2015), including analytical methods  
223 and QA/QC for lithogeochemical data. Lithogeochemical data are reproduced here only  
224 to compare to Nd isotope results.

### 225 *Neodymium isotopes*

226 Twelve representative samples in total were selected for Nd isotopic determinations,  
227 including ten exhalites from the three main exhalite types and 2 tuffs that are intercalated  
228 with the exhalites (Fig. 4A-F). These samples were chosen to cover both the horizontal  
229 and vertical distributions of all exhalite types and tuff occurring in the Lemarchant area.  
230 Additionally, one least altered sample of the felsic and mafic volcanic rocks (Fig. 4G-H)

231 were selected for analyses, and for comparison to exhalite samples. Samarium and Nd  
232 isotopic compositions were measured at Memorial University using a multicollector  
233 Finnigan MAT 262 thermal ionization mass spectrometer (TIMS) in static and dynamic  
234 acquiring modes. Samples for Nd analyses were prepared using the methods of Fisher *et*  
235 *al.* (2011) from whole-rock powders using a multi-acid (HF, HNO<sub>3</sub>, and HCl)  
236 dissolution-evaporation process. Separation of Sm and Nd was obtained using  
237 conventional two-step column chemical methods (Fisher *et al.* 2011).

238

239 Accuracy and precision for the Nd analyses were determined using the standards JNdi-1  
240 and BCR-2 as reference materials following methods described in Fisher *et al.* (2011).

241 The JNdi-1 and BCR-2 standards have following reported values: <sup>143</sup>Nd/<sup>144</sup>Nd =  
242 0.512115 and <sup>143</sup>Nd/<sup>144</sup>Nd = 0.512633, respectively (Tanaka *et al.* 2000; Raczek *et al.*  
243 2003). Standards were run every 11 samples with each analytical batch. Additionally,  
244 blanks were utilized during each analytical run to test contamination; none was detected.  
245 Precision was determined using the percent relative standard deviation (%RSD) on the  
246 replicate analyses of the reference materials, and accuracy was determined using percent  
247 relative difference (%RD) from accepted values. Analyses for the Lemarchant samples  
248 have an average 0.0013 %RSD for <sup>143</sup>Nd/<sup>144</sup>Nd and 0.00055 %RD for <sup>143</sup>Nd/<sup>144</sup>Nd.

249

250 The results herein are presented using the epsilon notation (εNd) and calculated for a  
251 formation age of 513 Ma, the U-Pb age of the host stratigraphy as reported by Dunning *et*  
252 *al.* (1991); data are presented in Table 1 and Figures 4B, 5A-B, and Figure 8. εNd<sub>513</sub> was  
253 calculated by  $\epsilon Nd_t = \left( \frac{{}^{143}\text{Nd}/{}^{144}\text{Nd}_{\text{rock,t}}}{{}^{143}\text{Nd}/{}^{144}\text{Nd}_{\text{CHUR,t}}} \right) \times 10^4$  after Rollinson (1993)

254 and  $f^{Sm/Nd} = [(^{147}Sm/^{144}Nd_{sample,t}) / (^{147}Sm/^{144}Nd_{CHUR,t}) - 1]$  after McLennan *et al.* (1990).  
255 Chondrite uniform reservoir (CHUR) values utilized in this study are  $^{143}Nd/^{144}Nd$  of  
256 0.512638 and a  $^{147}Sm/^{144}Nd$  of 0.1967 (Hamilton *et al.* 1983; Rollinson 1993). Depleted  
257 mantle model ages ( $T_{DM}$ ) were calculated using depleted mantle values of  $^{144}Nd/^{144}Nd =$   
258 0.513163 and  $^{147}Sm/^{144}Nd = 0.2137$ , and a decay constant of  $\lambda = 6.54 \times 10^{-12}$  (Goldstein  
259 *et al.* 1984).

## 260 *Results*

261 *Neodymium isotopic systematics.* The Lemarchant exhalites (n = 10) have  $\epsilon Nd_{513}$   
262 = -6.0 to -1.8 and  $T_{DM} = 1.63$  to 3.05 Ga (Table 1). Overall, the three types of  
263 Lemarchant exhalites (EMS = proximal; FEM = distal; IFE = interflow) have similar  
264  $\epsilon Nd_{513}$  values; however, the EMS-type have slightly lower  $\epsilon Nd_{513}$  values and range from  
265 -5.6 to -4.1 with an average of -4.8; the FEM-type are less evolved and range from  
266  $\epsilon Nd_{513} = -4.0$  to -3.2 with an average of -3.7; and the IFE-type has the widest range of  
267  $\epsilon Nd_{513} = -6.0$  to -1.8 and average of -3.9 (Table 1; Fig. 6B, 7A-B). The Lemarchant tuff  
268 samples (n = 2) have  $\epsilon Nd_{513} = -5.7$  to -4.7 with an average of -5.2 and  $T_{DM} = 1.75$  to  
269 1.81 Ga. In  $\epsilon Nd$  versus Th/Sc space the Lemarchant exhalites and tuff have Th/Sc ratios  
270 of 0.06 to 1.93 and fall between the arc andesite fields, with samples that have greater  
271 Th/Sc containing lower  $\epsilon Nd$  values similar to upper crust values (Fig. 7A). These more  
272 evolved samples also trend towards the field of the 563 Ma Crippleback Intrusive Suite  
273 and Sandy Brook Group basement rocks (recalculated here at 513 Ma for comparison;  
274 Fig. 7A). The Lemarchant felsic and mafic volcanic rock measured in this study have  
275  $\epsilon Nd_{513} = +0.4$  and a  $T_{DM} = 1.47$  Ga, and  $\epsilon Nd_{513} = +1.4$  and a  $T_{DM} = 1.74$  Ga, respectively,  
276 and plot in the field for arc rocks (Table 1; Fig. 7B). These values for the Lemarchant

277 volcanic rocks are similar to values reported by Rogers *et al.* (2006) and McNicoll *et al.*  
278 (2010) for felsic and mafic volcanic rocks of the Tally Pond volcanic belt, including  
279 samples from the ‘Upper Block’ and the ‘Mineralized Block’ of the Duck Pond deposit  
280 (Fig. 7B).

281

282 The  $f^{\text{Sm/Nd}}$  reflects the fractional deviation of  $^{147}\text{Sm}/^{144}\text{Nd}$  from CHUR in parts per  $10^4$   
283 because of light rare earth element enrichment (i.e., lower Sm/Nd) during igneous  
284 differentiation processes (McLennan *et al.* 2003). Accordingly, in  $f^{\text{Sm/Nd}}$ - $\epsilon\text{Nd}$  space (Fig.  
285 7B) the Lemarchant exhalite and tuff samples have more evolved  $\epsilon\text{Nd}_{513}$  values than the  
286 Lemarchant volcanic rocks, and are comparable to values reported by Rogers *et al.*  
287 (2006) for the Neoproterozoic Crippleback quartz monzonite and Sandy Brook Group  
288 rhyolite. However, the Lemarchant exhalite and tuff samples have  $f^{\text{Sm/Nd}}$  higher than the  
289 Neoproterozoic Crippleback quartz-monzonite and Sandy Brook Group rhyolite and  
290 trend towards those of the Tally Pond group volcanic rocks (Fig. 7B; McLennan *et al.*  
291 2003). The  $\epsilon\text{Nd}$  values of the Lemarchant exhalite and tuff samples do not show any  
292 spatial variations throughout the zones of the deposit and/or with depth in the stratigraphy  
293 in the Lemarchant area (Fig. 6A-B). The  $T_{\text{DM}} = 1.63$  to 3.05 Ga of the Lemarchant  
294 exhalites are older than reported values for the coeval felsic volcanic rocks of the ‘Upper  
295 Block’ and ‘Mineralized Block’ at Duck Pond of 1.06 and 1.35 Ga, and 0.95 Ga,  
296 respectively (McNicoll *et al.* 2010), and those of the Crippleback Intrusive Suite (1.26  
297 and 1.35 Ga) and the Sandy Brook Group (1.15 to 1.34 Ga; Rogers *et al.* 2006; this  
298 study).

299            *Immobile element systematics*: Volcanic rocks of the Tally Pond group that are  
300 associated with the hydrothermal sedimentary rocks and volcanic and igneous rocks of  
301 the Sandy Brook Group and Crippleback Intrusive Suites are shown on the immobile  
302 element Zr/Ti-Nb/Y classification diagram by Winchester and Floyd (1977) and Pearce  
303 (1996) in Figure 8. This plot enables to discriminate and identify rock types,  
304 independently from the degree of alteration (Winchester & Floyd 1977; Pearce 1996).  
305 The volcanic rocks from the Lemarchant deposit are subalkaline basaltic andesites, with  
306 the more felsic rocks trending towards dacite boundary, and the more mafic rocks  
307 trending towards the basalt boundary (Fig. 8). Because of the limited sample number for  
308 volcanic rocks from this study, fields from Cloutier *et al.* (2017) were added for felsic,  
309 intermediate, and mafic volcanic rocks from the Lemarchant deposit (Fig. 8).  
310 Additionally, samples for Tally Pond group felsic and mafic volcanic rocks, the Sandy  
311 Brook Group rhyolite and basalt and Crippleback quartz monzonite of Rogers (2004) and  
312 Rogers et al (2006) were also added for comparison. Chemically, the volcanic rocks of  
313 Lemarchant show a wide distribution, with felsic-dominated rhyolite-dacites of the  
314 Bindons Pond formation as well as intermediate andesite-basaltic andesites and mafic  
315 rocks of the Lake Ambrose formation (Cloutier *et al.* 2017), which is consistent with  
316 potential source rocks for the detrital constituent in the hydrothermal sedimentary rocks  
317 and regional models for the Tally Pond group (e.g., Rogers *et al.* 2007; Piercey *et al.*  
318 2014).

319

## 320 **Discussion**

321 *Provenance, tectonic setting, and the role of crustal input*

322 The Tally Pond group represents the oldest magmatism of the Penobscot Arc and was  
323 developed during phases of arc rifting at the leading edge of the Ganderian margin  
324 (Rogers *et al.* 2006; Zagorevski *et al.* 2010; Piercey *et al.* 2014).  
325 Penecontemporaneously, further rifting on the trailing edge of Ganderia, led to the  
326 formation of the Ellsworth belt (~509-505 Ma) of coastal Maine and New Brunswick  
327 representing the separation of Ganderia from the Gondwanan Amazonian margin (Fyffe  
328 *et al.* 2009; van Staal *et al.* 2012). The volcanic rocks of the Ellsworth terrane comprise  
329 tholeiitic basalts and rhyolites with  $\epsilon\text{Nd}_{500 \text{ Ma}}$  values ranging from +5.6 to +8.6, but also  
330 calc-alkaline rhyolite (R-1 Rhyolite) that yielded  $\epsilon\text{Nd}_{500 \text{ Ma}} \sim 0$  (Schulz *et al.* 2008). The  
331 latter are similar to the  $\epsilon\text{Nd}$  values of felsic and mafic volcanic rock samples from the  
332 Tally Pond group (Bindons Pond and Lake Ambrose formations) of this study ( $\epsilon\text{Nd} =$   
333 +1.4 and +0.4, respectively), which are comparable with values that were previously  
334 reported for the Tally Pond group volcanic rocks (Fig. 7B; Rogers *et al.* 2006; Zagorevski  
335 *et al.* 2010). This illustrates that the Lake Ambrose formation basalts have predominantly  
336 juvenile signatures ( $\epsilon\text{Nd}_{511 \text{ Ma}} = +3$ ; Rogers *et al.* 2006 and this study), whereas Bindons  
337 Pond formation rhyolites and dacites have less juvenile values ( $\epsilon\text{Nd}_{511 \text{ Ma}} = +1.8$  and +2.6)  
338 (Rogers *et al.* 2006; Zagorevski *et al.* 2010). There is a noticeable difference in  $\epsilon\text{Nd}_{513 \text{ Ma}}$   
339 values between the sedimentary and volcanic rocks of the Lemarchant deposit, however.  
340 In general, the exhalites and tuffs have lower  $\epsilon\text{Nd}_{513}$  values ranging from  $-6.0$  to  $-1.8$   
341 (Fig. 7A-B), like the Sandy Brook Group rhyolite  $\epsilon\text{Nd}_{513 \text{ Ma}} = -6.5$  to  $-1.9$ , and the  
342 Crippleback Intrusive Suite  $\epsilon\text{Nd}_{513 \text{ Ma}} = -5.9$  to  $-5.2$  (Rogers *et al.* 2006). Mafic volcanic  
343 rocks are common in the Sandy Brook Group; however, no Nd isotopic data are  
344 published thus no comparison can be made to data from this study. Kerr *et al.* (1995)

345 presented data for Late Precambrian mafic rocks of the Valentine Lake Pluton, which is  
346 correlative to the Crippleback Intrusive Suite, and may also represent a correlative mafic  
347 unit to the Sandy Brook Group mafic rocks (Kerr *et al.* 1995). The Valentine Lake Pluton  
348 mafic rocks yielded an  $\epsilon\text{Nd}_{570 \text{ Ma}}$  of +0.5 (Kerr *et al.* 1995). Given the similarities to  
349 Tally Pond mafic rocks, it is not possible to clearly distinguish the Late Precambrian  
350 mafic rocks from the Cambrian mafic volcanic rocks of the Tally Pond group.

351 Considering that the exhalites, regardless of the exhalite type (proximal, distal,  
352 interflow), have negative  $\epsilon\text{Nd}_t$  values, contributions from mafic sources from either the  
353 Tally Pond group or underlying Sandy Brook Group appear minimal and negligible.

354

355 There are a number of potential Nd sources in hydrothermal sedimentary rocks  
356 (exhalites), including seawater-derived/scavenged, detrital, and hydrothermally-derived  
357 components (Goldstein *et al.* 1984; Mills *et al.* 1993; Mills & Elderfield 1995).  
358 Scavenging of REE from seawater occurs during mixing of the hydrothermal fluids with  
359 seawater, where oxyanions (e.g.,  $\text{HPO}_4^{2-}$ ,  $\text{HVO}_4^{2-}$ ,  $\text{CrO}_4^{2-}$ ,  $\text{HAsO}_4^{2-}$ ), trace elements, and  
360 rare earth elements (REE, including Nd) are scavenged from seawater onto Fe-  
361 oxyhydroxides, and subsequently deposited around the hydrothermal vent site (de Baar *et*  
362 *al.* 1988; Rudnicki 1995; German & Von Damm 2003; Peter 2003). Nd isotopic  
363 signatures measured from modern seawater show a wide range that indicate that  
364 continental Nd is the predominant source of REE in modern seawater resulting in  
365 different Nd values within the main water masses/oceans (Goldstein *et al.* 1984; Bertram  
366 & Elderfield 1993; Tachikawa *et al.* 2003). Thus, exposure of crustal basement during arc  
367 rifting would bring crustally-derived evolved Nd into the ambient seawater, together with



368 Nd derived from the broadly contemporaneously eruptions and erosion of the more  
369 juvenile Cambrian Tally Pond group volcanic rocks. Both sources of Nd would allow for  
370 scavenging of Nd that is dissolved in the water column via adsorption, or via a particulate  
371 Nd shuttle as detrital grains (e.g., detrital monazite; Wood & Williams-Jones 1994; Mills  
372 & Elderfield 1995; Rudnicki 1995; Chavagnac *et al.* 2005). In contrast, hydrothermal Nd  
373 is a minimal component in hydrothermal sediment, mostly because REE are in extremely  
374 low concentrations in seafloor hydrothermal fluids and initial hydrothermal Nd signatures  
375 in the hydrothermal sediment are often rapidly overprinted by Nd scavenged from  
376 seawater (Elderfield *et al.* 1988; Mills *et al.* 1993; Mills & Elderfield 1995).

377

378 Considering these processes and potential Nd sources, it is noticeable that even though  
379 the Lemarchant hydrothermal sediments predominantly consist of hydrothermally-  
380 derived matter (e.g., Zn-Pb-Cu-Fe-S), their Nd budget contains only minor  
381 hydrothermally-derived Nd. The dilution of hydrothermal fluids by seawater, scavenging  
382 processes, and contributions of detrital matter generally annihilates the initial  
383 hydrothermal Nd signatures in hydrothermal sediments (Mills & Elderfield 1995). In  
384 rifted arc basins, typical of that hosting the Lemarchant deposit (e.g., Cloutier *et al.*  
385 2017), the provenance of Nd is generally restricted and often local (i.e., Tally Pond group  
386 volcanic rocks, Crippleback Intrusive Suite and Sandy Brook Group basement rocks),  
387 such that erosion of these rocks results in locally-derived detrital Nd in the hydrothermal  
388 sedimentary rocks, as well as dissolved Nd in the water column (Figs. 9A-B, 10). The Nd  
389 in the Lemarchant exhalites was derived predominantly from scavenging and detrital  
390 matter, which explains their evolved Nd signatures; signatures that are not present in the

391 more juvenile Tally Pond group volcanic rocks. Moreover, the Lemarchant exhalites have  
392 similar  $\epsilon\text{Nd}_{513 \text{ Ma}}$  values throughout the sections of the Lemarchant Main Zone, the  
393 Northwest and 24 zones, and the North Target (Fig. 6A-B), albeit proximal Lemarchant  
394 exhalites (EMS-type) have more evolved  $\epsilon\text{Nd}_{513}$  values than the more distal exhalites  
395 (FEM-type; Figs. 6A-B). It is suggested that the more evolved Nd signatures of the  
396 proximal exhalites represent early stages of arc-rifting, which were dominated by erosion  
397 of the rifted Neoproterozoic Ganderian (see below) and possibly older crustal basement,  
398 whereas the more distal exhalites reflect greater contributions from the continuously  
399 erupting and erosion of the more juvenile Cambrian Tally Pond group volcanic rocks  
400 (Fig. 9A-B).

401

402 Significant input from crustal material is further supported by the Pb isotopic data of the  
403 Lemarchant deposit and other massive sulphide occurrences in the Tally Pond group  
404 (Swinden & Thorpe 1984; Pollock & Wilton 2001; Gill 2015; Lode *et al.* 2017).

405 Volcanogenic massive sulphides and associated hydrothermal sediments have Pb sources  
406 that derive their Pb predominantly from leaching of basement rocks, which may include  
407 different reservoirs (Franklin *et al.* 1981; Swinden & Thorpe 1984; Tosdal *et al.* 1999;  
408 Ayuso *et al.* 2003). Lead isotopic data measured *in-situ* on galena hosted within sulphides  
409 in the hydrothermal sediments using secondary ion mass spectrometry (SIMS), suggested  
410 hydrothermally- and detritally-derived Pb sources (Lode *et al.* 2017). Especially more  
411 vent distal exhalites showed more radiogenic detritally Pb contributions, which were  
412 characterised by more radiogenic  $^{206}\text{Pb}/^{204}\text{Pb}$  and  $^{208}\text{Pb}/^{204}\text{Pb}$  ratios (Mills & Elderfield  
413 1995; Lode *et al.* 2017). These data are also consistent with derivation of Pb from

414 juvenile to evolved sources and suggest such crust was present beneath the Tally Pond  
415 group.  
416

417 The Nd and Pb isotopic data from Lemarchant exhalites also provide insight into the  
418 crustal architecture and potential palaeogeographic relationships of the Lemarchant  
419 deposit and Tally Pond group within the Iapetus Ocean. For example, inherited zircons  
420 (563 Ma) in the Cambrian felsic volcanic rocks of the Tally Pond group are consistent  
421 with them having erupted from or interacted with Neoproterozoic Ganderian basement  
422 rocks (Crippleback Intrusive Suite and the coeval bimodal Sandy Brook Group; Rogers *et al.*  
423 *al.* 2006; Rogers *et al.* 2007; McNicoll *et al.* 2010; Zagorevski *et al.* 2010). Similar,  
424 Neoproterozoic (~553 Ma) inherited zircon ages are also known from rocks of the Pats  
425 Pond group (~487 Ma), which are found regionally proximal to the Tally Pond group  
426 albeit younger, and these rocks also have Mesoproterozoic (0.9-1.2 Ga) xenocrystic  
427 zircons (Zagorevski *et al.* 2007, Zagorevski *et al.* 2010). This indicates that the bimodal  
428 Pats Pond group was built near or upon Ganderian basement as the Tally Pond group  
429 (Zagorevski *et al.* 2010). Plutonic and gneissic boulders, as well as sedimentary rocks in  
430 the Ellsworth Formation of coastal Maine and New Brunswick, rocks  
431 penecontemporaneous with the Tally Pond group, contained small populations of  
432 Mesoproterozoic, Palaeoproterozoic, and Archean zircons up to 3.23 Ga, but with a  
433 dominant population between 1.07 to 1.61 Ga (Hibbard *et al.* 2007; Schulz *et al.* 2008;  
434 Fyffe *et al.* 2009; van Staal *et al.* 2012). These inherited zircon patterns present in the  
435 Victoria Lake supergroup and Ellsworth terrane are consistent with these rocks being  
436 built atop Ganderian basement, and are also consistent with Ganderia having originated

437 along the Gondwanan Amazonian margin (Fyffe *et al.* 2009; van Staal *et al.* 2012). The  
438 Mesoproterozoic to Archean  $T_{DM}$  model ages and Nd isotopic data of the Lemarchant  
439 exhalites (1.63 to 3.05 Ga) together with the detrital zircon populations and the Nd  
440 signatures of the Tally Pond group volcanic rocks, as well as of the Crippleback Intrusive  
441 Suite and Sandy Brook Group, are also consistent with an Amazonian provenance for  
442 Ganderia, and also suggests that the Tally Pond group evolved along this margin (Fig. 8;  
443 Zagorevski *et al.* 2007; Pollock *et al.* 2011; van Staal & Barr 2011; van Staal *et al.* 2012).

444

445 Altogether, the Nd and Pb isotopic data support that older crustal basement plays a role in  
446 hydrothermal activity in the Tally Pond group, either through direct leaching (Pb), detrital  
447 (Pb+Nd), or via adsorption/deposition from the water column (Nd). Furthermore, trace  
448 element signatures of the Tally Pond group volcanic rocks and provenance-related  
449 immobile element systematics of the exhalites are consistent with a formation in a  
450 volcanic arc environment, such as a graben/caldera in a rifted continental arc, or an arc  
451 proximal to continental crust along the Gondwanan margin (Rogers *et al.* 2006;  
452 Zagorevski *et al.* 2010; Piercey *et al.* 2014). Therefore, exhalites that precipitate in a  
453 rifted arc basin/caldera setting record diverse provenance components that are useful for  
454 palaeogeographic reconstructions and provide a mechanism to elucidate the source of  
455 metals that contributed to the formation of spatially and genetically associated massive  
456 sulphides.

457

458 **Conclusions**

459 It is proposed that the volcanogenic massive sulphides of the Lemarchant deposit and  
460 related exhalites formed from fluids that ascended along deep synvolcanic faults in a  
461 rifted arc basin that contained Cambrian (~513-509 Ma) felsic, intermediate, and mafic  
462 volcanic rocks and was underlain by Neoproterozoic (~565 Ma) mafic and felsic volcanic  
463 rocks (Sandy Brook Group), and associated intrusive rocks (Crippleback Lake Intrusive  
464 Suite). The eruption and erosion of the Tally Pond group volcanic rocks within this rift-  
465 related graben/caldera environment resulted in the addition of juvenile Nd to the basin  
466 and water column that was recorded in the exhalites that are found near massive sulphide  
467 mineralization. Furthermore, the uplift associated with arc rifting led to the erosion of the  
468 Ganderian arc rocks of the Crippleback Intrusive Suite and the coeval Sandy Brook  
469 Group resulting in the addition of evolved crustal Nd to both ambient seawater and as  
470 detrital materials. Exhalative sedimentary rocks in the Lemarchant deposit contain both  
471 Nd scavenged from seawater and from detritus and they collectively record Nd additions  
472 from both Neoproterozoic Ganderian basement and intrabasinal Tally Pond group  
473 volcanic sources. These results are also consistent with previous detrital zircon and Nd  
474 isotopic studies that suggest that unexposed older crustal basement of the Gondwanan  
475 Amazonian margin existed beneath the Ganderian arc rocks and contributed detrital Nd to  
476 the Tally Pond group and Lemarchant exhalites specifically. As the precipitating  
477 exhalites record the mixed sources, with evolved and juvenile  $\epsilon\text{Nd}$  signatures, the  
478 abundance of exhalites with more evolved  $\epsilon\text{Nd}$  systematics suggests that the predominant  
479 source of Nd was eroded older crustal material. However, results herein and published  
480 previously suggest that this Amazonian basement signature is not recorded significantly  
481 in the volcanic rocks of the Tally Pond group. Overall, the Nd isotopic compositions, as

482 well as the lithogeochemical data, of the Lemarchant exhalites suggests that the  
483 Lemarchant deposit exhalites record a formation within a rifted arc environment built  
484 upon Ganderian (exposed) and Gondwanan Amazonian (unexposed) crustal basement,  
485 consistent with existing models for the Tally Pond group.

486

#### 487 **Acknowledgements**

488 Kind support was provided by Dianne and Charlie Fost, Michael Vande Guchte,  
489 Alexandria Marcotte, and Gerry Squires from Paragon Minerals Corporation (a 100%-  
490 owned subsidiary of Canadian Zinc Corporation). The authors would further like to thank  
491 Keir Hiscock, Pam King, Sherry Strong, Anne Westhues, as well as Luke Beranek and  
492 Greg Dunning for the helpful reviews and Inês Nobre Silva for general discussions, help,  
493 and support. Furthermore, the authors are thankful for the thoughtful comments and  
494 suggestions of the reviewers, Neil Rogers and the anonymous reviewer, and the subject  
495 editor of the *Journal of the Geological Society*, Anna Frances Bird.  
496

#### 497 **Funding information**

498 Research funded by the Canadian Mining Research Organization (CAMIRO, Project  
499 08E04) and grants of the Natural Sciences and Engineering Research Council of Canada  
500 (NSERC): NSERC Discovery Grant – 249695-2011; NSERC IRC Grant – 408433-09;  
501 NSERC CRD Grant – CAMIRO Project – CRDPJ 387592-09; RDC and a grant of the  
502 Research and Development Corporation of Newfoundland and Labrador (RDC) RDC  
503 IRIF for IRC – 5003.121.001 to Dr. Stephen Piercey. Research was also funded by the  
504 NSERC-Altius Industrial Research Chair in Mineral Deposits, funded by NSERC, Altius  
505 Resources Inc.

506

#### 507 **References**

- 508 Ayuso, R.A. & Schulz, K.J. 2003. Nd-Pb-Sr isotope geochemistry and origin of the  
509 Ordovician Bald Mountain and Mount Chase massive sulfide deposits, northern Maine.  
510 *Economic Geology Monographs*, **11**, 611-630.  
511  
512 Bertram, C.J. & Elderfield, H. 1993. The geochemical balance of the rare earth elements  
513 and neodymium isotopes in the oceans. *Geochimica et Cosmochimica Acta*, **57**, 1957-  
514 1986.  
515  
516 Boström, K. 1973. The Origin and Fate of Ferromanganoan Active Ridge Sediments.  
517 *Stockholm Contributions In Geology*, **27**, 147-243.  
518

519 Boström, K., Joensuu, O., Valdés, S. & Riera, M. 1972. Geochemical history of South  
520 Atlantic Ocean sediments since Late Cretaceous. *Marine Geology*, **12**, 85-121, doi:  
521 [http://dx.doi.org/10.1016/0025-3227\(72\)90023-0](http://dx.doi.org/10.1016/0025-3227(72)90023-0).  
522

523 Boström, K. & Peterson, M.N.A. 1969. The origin of aluminum-poor ferromanganoan  
524 sediments in areas of high heat flow on the East Pacific Rise. *Marine Geology*, **7**, 427-  
525 447, doi: [http://dx.doi.org/10.1016/0025-3227\(69\)90016-4](http://dx.doi.org/10.1016/0025-3227(69)90016-4).  
526

527 Chavagnac, V., German, C.R., Milton, J.A. & Palmer, M.R. 2005. Sources of REE in  
528 sediment cores from the Rainbow vent site (36°14'N, MAR). *Chemical Geology*, **216**,  
529 329-352, doi: 10.1016/j.chemgeo.2004.11.015.  
530

531 Cloutier, J., Piercey, S.J., Lode, S., Vande Guchte, M. & Copeland, D.A. 2017.  
532 Lithostratigraphic and structural reconstruction of the Zn-Pb-Cu-Ag-Au Lemarchant  
533 volcanogenic massive sulphide (VMS) deposit, Tally Pond group, central Newfoundland,  
534 Canada. *Ore Geology Reviews*, **84**, 154-173.  
535

536 Copeland, D.A. 2009. Assessment Report on Prospecting, Lithochemical Sampling  
537 and Data Interpretation on the Harpoon Property (Licenses 7695M, 10461M, 10464M,  
538 10465M, 10607M, 12357M, 12885M, 13583M, 13448M, 13449M and 13667M) and the  
539 South Tally Pond Property (Licences 8183M, 9569M and 14158M) Lake Ambrose Area,  
540 Newfoundland and Labrador. **NTS 12A/10 and 12A/07**. Paragon Minerals Corporation.  
541

542 Copeland, D.A., Toole, R.M. & Piercey, S.J. 2009. 10th Year Supplementary Assessment  
543 Report on Soil Sampling, Linecutting, Titan 24 Geophysical Surveying, Diamond  
544 Drilling and Petrography, Licence 8183M, South Tally Pond Property, Rogerson Lake  
545 Area, Newfoundland and Labrador, NTS 12A/10 and 12A/07. *Newfoundland and*  
546 *Labrador Geological Survey Assessment File*.  
547

548 de Baar, H.J.W., German, C.R., Elderfield, H. & van Gaans, P. 1988. Rare earth element  
549 distributions in anoxic waters of the Cariaco Trench. *Geochimica et Cosmochimica Acta*,  
550 **52**, 1203-1219.  
551

552 DePaolo, D.J. 1981. Neodymium isotopes in the Colorado Front Ranges and crust-mantle  
553 evolution in the Proterozoic. *Nature*, **291**, 193-196, doi: doi:10.1038/291193a0.  
554

555 Dunning, G.R., Kean, B.F., Thurlow, J.G. & Swinden, H.S. 1987. Geochronology of the  
556 Buchans, Roberts Arm, and Victoria Lake groups and Mansfield Cove Complex,  
557 Newfoundland. *Canadian Journal of Earth Sciences*, **24**, 1175-1184.  
558

559 Dunning, G.R., Swinden, H.S., Kean, B.F., Evans, D.T.W. & Jenner, G.A. 1991. A  
560 Cambrian island arc in Iapetus; geochronology and geochemistry of the Lake Ambrose  
561 volcanic belt, Newfoundland Appalachians. *Geological Magazine*, **128**, 1-17.  
562

563 Elderfield, H., Charnock, H., Lovelock, J.E., Liss, P.S. & Whitfield, M. 1988. The  
564 oceanic chemistry of the rare-earth elements. *Philosophical Transactions of the Royal*  
565 *Society of London, Series A: Mathematical and Physical Sciences*, **325**, 105-124.  
566

567 Evans, D.T.W. & Kean, B.F. 2002. The Victoria Lake Supergroup, central Newfoundland  
568 - its definition, setting and volcanogenic massive sulphide mineralization. *Newfoundland*  
569 *and Labrador Department of Mines and Energy, Geological Survey, Open File*  
570 *NFLD/2790*.  
571

572 Evans, D.T.W., Kean, B.F. & Dunning, G.R. 1990. Geological Studies, Victoria Lake  
573 Group, Central Newfoundland *Current Research Report, Geological Survey Branch,*  
574 *Report: 90-1*, 131-144.  
575

576 Fisher, C.M., McFarlane, C.R.M., Hanchar, J.M., Schmitz, M.D., Sylvester, P.J., Lam, R.  
577 & Longerich, H.P. 2011. Sm-Nd isotope systematics by laser ablation-multicollector-  
578 inductively coupled plasma mass spectrometry: Methods and potential natural and  
579 synthetic reference materials. *Chemical Geology*, **284**, 1-20.  
580

581 Franklin, J.M., Sangster, D.M. & Lydon, J.W. 1981. Volcanic-associated massive sulfide  
582 deposits. In: Skinner, B.J. (ed.) *Economic Geology Seventy-Fifth Anniversary Volume*.  
583 Society of Economic Geologists, 485-627.  
584

585 Fraser, D., Giroux, G.A., Copeland, D.A. & Devine, C.A. 2012. *NI-43-101* Technical  
586 Report and Mineral Resource Estimate on the Lemarchant Deposit, South Tally Pond  
587 VMS Project, central Newfoundland, Canada for Paragon Minerals Corporation. *National*  
588 *Instrument 43-101 Technical Report*.  
589

590 Fyffe, L.R., Barr, S.M., Johnson, S.C., McLeod, M.J., McNicoll, V.J., Valverde-Vaquero,  
591 P., van Staal, C.R. & White, C.E. 2009. Detrital zircon ages from Neoproterozoic and  
592 Early Proterozoic conglomerate and sandstone units of New Brunswick and coastal  
593 Maine: implications for the tectonic evolution of Ganderia. *Atlantic Geology*, **45**, 110-  
594 144.  
595

596 Gale, A., Langmuir, C.H. & Dalton, C.A. 2014. The global systematics of Ocean Ridge  
597 Basalts and their origin. *Journal of Petrology*, **55**, 1051-1082.  
598

599 Galley, A.G., Hannington, M. & Jonasson, I. 2007. Volcanogenic massive sulphide  
600 deposits. In: Goodfellow, W.D. (ed.) *Mineral Deposits of Canada: A Synthesis of Major*  
601 *Deposit-types, District Metallogeny, the Evolution of Geological Provinces, and*  
602 *Exploration Methods*. Special Publication 5, Mineral Deposits Division, Geological  
603 Association of Canada, 141-161.  
604

605 German, C.R. & Von Damm, K.L. 2003. Hydrothermal Processes. *Treatise on*  
606 *Geochemistry*. Pergamon, Oxford, 181-222.  
607



608 Gibson, H.L., Allen, R.L., Riverin, G. & Lane, T.E. 2007. The VMS model: Advances  
609 and application to exploration targeting. *In: Milkereit, B. (ed.) Proceedings of*  
610 *Exploration 07: Fifth Decennial International Conference on Mineral Exploration,*  
611 *Toronto, ON, 717-730.*  
612  
613 Gill, S.B. 2015. Mineralogy, metal zoning, and genesis of the Zn-Pb-Ba-Ag-Au  
614 Lemarchant volcanogenic massive sulfide (VMS) deposit. *M.Sc. Thesis*, Memorial  
615 University of Newfoundland.  
616  
617 Goldstein, S.L., O'Nions, R.K. & Hamilton, P.J. 1984. A Sm-Nd isotopic study of  
618 atmospheric dusts and particulates from major river systems. *Earth and Planetary*  
619 *Science Letters*, **70**, 221-237.  
620  
621 Grenne, T. & Slack, J.F. 2003. Bedded jaspers of the Ordovician Lokken Ophiolite,  
622 Norway; seafloor deposition and diagenetic maturation of hydrothermal plume-derived  
623 silica-iron gels. *Mineralium Deposita*, **38**, 625-639.  
624  
625 Hamilton, P.J., O'Nions, R.K., Bridgwater, D. & Nutman, A. 1983. Sm-Nd studies of  
626 Archaean metasediments and metavolcanics from West Greenland and their implications  
627 for the Earth's early history. *Earth and Planetary Science Letters*, **63**, 263-273.  
628  
629 Hannington, M.D. 2014. Volcanogenic massive sulfide deposits. *In: Holland, H.D., and*  
630 *Turekian, K.K. (ed.) Treatise on Geochemistry 2nd Edition.* Elsevier Ltd, Reviews in  
631 *Economic Geology*, **13** 319-350.  
632  
633 Hannington, M.D., de Ronde, C.E.J. & Petersen, S. 2005. Sea floor tectonics and  
634 submarine hydrothermal systems. *In: Hedenquist, J.W., Thompson, J.F.H., Goldfarb, R.J.*  
635 *& Richards, J.P. (eds.) Economic Geology: One Hundredth Anniversary Volume, 1905-*  
636 *2005.* Society of Economic Geologists, Littleton, CO, USA, 111-142.  
637  
638 Hannington, M.D., Jonasson, I.R., Herzig, P.M. & Petersen, S. 1995. Physical and  
639 chemical processes of seafloor mineralization at mid-ocean ridges. *Geophysical*  
640 *Monograph*, **91**, 115-157.  
641  
642 Hawkesworth, C.J., Norry, M.J., Baker, R.P.E., Francis, P.W. & Thorpe, R.S. 1979.  
643  $^{143}\text{Nd}/^{144}\text{Nd}$ ,  $^{87}\text{Sr}/^{86}\text{Sr}$ , and incompatible element variations in calc-alkaline andesites  
644 and plateau lavas from South America. *Earth and Planetary Science Letters*, **42**, 45-57.  
645  
646 Hekinian, R., Hoffert, M., Larqué, P., Cheminée, J.L., Stoffers, P. & Bideau, D. 1993.  
647 Hydrothermal Fe and Si oxyhydroxide deposits from South Pacific intraplate volcanoes  
648 and East Pacific Rise axial and off-axial regions. *Economic Geology*, **88**, 2099-2121.  
649  
650 Hibbard, J.P., van Staal, C.R. & Rankin, D.W. 2007. A comparative analysis of pre-  
651 Silurian crustal building blocks of the northern and the southern Appalachian orogen.  
652 *American Journal of Science*, **307**, 23-45, doi: 10.2475/01.2007.02.  
653

654 Hollis, S.P., Cooper, M.R., Herrington, R.J., Roberts, S., Earls, G., Verbeeten, A.,  
655 Piercey, S.J. & Archibald, S.M. 2015. Distribution, mineralogy and geochemistry of  
656 silica-iron exhalites and related rocks from the Tyrone Igneous Complex: Implications  
657 for VMS mineralization in Northern Ireland. *Journal of Geochemical Exploration*, **159**,  
658 148-168, doi: <http://dx.doi.org/10.1016/j.gexplo.2015.09.001>.  
659

660 Huston, D.L., Pehrsson, S., Eglington, B.M. & Zaw, K. 2010. The geology and  
661 metallogeny of volcanic-hosted massive sulfide deposits: Variations through geologic  
662 time and with tectonic setting. *Economic Geology*, **105**, 571-591, doi:  
663 10.2113/gsecongeo.105.3.571.  
664

665 Huston, D., Relvas, J., Gemmell, J. & Driberg, S. 2011. The role of granites in volcanic-  
666 hosted massive sulphide ore-forming systems: an assessment of magmatic–hydrothermal  
667 contributions. *Mineralium Deposita*, **46**, 473-507, doi: 10.1007/s00126-010-0322-7.  
668

669 Ickert, R.B. 2013. Algorithms for estimating uncertainties in initial radiogenic isotope  
670 ratios and model ages. *Chemical Geology*, **340**, 131-138, doi:  
671 10.1016/j.chemgeo.2013.01.001.  
672

673 Jenner, G.A. & Swinden, H.S. 1993. The Pipestone Pond Complex, central  
674 Newfoundland; complex magmatism in an eastern Dunnage Zone ophiolite. *Canadian*  
675 *Journal of Earth Sciences*, **30**, 434-448.  
676

677 Kerr, A., Jenner, G.A. & Fryer, B.J. 1995. Sm-Nd isotopic geochemistry of Precambrian  
678 to Paleozoic granitoid suites and the deep-crustal structure of the southeast margin of the  
679 Newfoundland Appalachians. *Canadian Journal of Earth Sciences*, **32**, 224-245.  
680

681 Keto, L.S. & Jacobson, S.B. 1988. Nd isotopic variations of Phanerozoic palaeoceans.  
682 *Earth and Planetary Science Letters*, **90**, 395-410.  
683

684 Lode, S., Piercey, J.S. & Devine, C.A. 2015. Geology, mineralogy, and  
685 litho-geochemistry of metalliferous mudstones associated with the Lemarchant  
686 volcanogenic massive sulfide deposit, Tally Pond belt, central Newfoundland. *Economic*  
687 *Geology*, **110**, 1835-1859.  
688

689 Lode, S., Piercey, S.J. & Squires, G.C. 2016. Role of metalliferous mudstones and  
690 detrital shales in the localization, genesis, and paleoenvironment of volcanogenic  
691 massive sulphide deposits of the Tally Pond volcanic belt, central Newfoundland,  
692 Canada. *Canadian Journal of Earth Sciences*, **53**, 387-425.  
693

694 Lode, S., Piercey, S.J., Layne, G.D., Piercey, G. & Cloutier, J. 2017. Multiple sulphur  
695 and lead sources recorded in hydrothermal exhalites associated with the Lemarchant  
696 volcanogenic massive sulphide deposit, central Newfoundland, Canada. *Mineralium*  
697 *Deposita*, **52**, 105-128, doi: 10.1007/s00126-016-0652-1.  
698

699 Lydon, J.W. 1984. Ore deposit models; 8, Volcanogenic sulphide deposits; Part I, A  
700 descriptive model. *Geoscience Canada*, **11**, 195-202.  
701

702 McCulloch, M.T. & Wasserburg, G.J. 1978. Sm-Nd and Rb-Sr chronology of continental  
703 crust formation. *Science*, **200**, 1003-1011.  
704

705 McLennan, S.M. 1989. Rare earth elements in sedimentary rocks; influence of  
706 provenance and sedimentary processes. *Reviews in Mineralogy*, **21**, 169-200.  
707

708 McLennan, S.M., Bock, B., Hemming, S.R., Hurowitz, J.A., Lev, S.M. & McDaniel,  
709 D.K. 2003. The roles of provenance and sedimentary processes in the geochemistry of  
710 sedimentary rocks. In: Lentz, D.R. (ed.) *Geochemistry of Sediments and Sedimentary*  
711 *Rocks: Evolutionary Considerations to Mineral Deposit-Forming Environments*.  
712 Geological Association of Canada, St. John's, NL, Canada, 7-38.  
713

714 McLennan, S.M., Hemming, S., McDaniel, D.K. & Hanson, G.N. 1993. Geochemical  
715 approaches to sedimentation, provenance, and tectonics. *Special Paper Geological*  
716 *Society of America*, **284**, 21-40.  
717

718 McLennan, S.M., Taylor, S.R., McCulloch, M.T. & Maynard, J.B. 1990. Geochemical  
719 and Nd-Sr isotopic composition of deep-sea turbidites; crustal evolution and plate  
720 tectonic associations. *Geochimica et Cosmochimica Acta*, **54**, 2015-2050.  
721

722 McNicoll, V., Squires, G., Kerr, A. & Moore, P. 2010. The Duck Pond and Boundary Cu-  
723 Zn deposits, Newfoundland: new insights into the ages of host rocks and the timing of  
724 VHMS mineralization. *Canadian Journal of Earth Sciences*, **47**, 1481-1506.  
725

726 Mills, R., Elderfield, H. & Thomson, A. 1993. A dual origin for the hydrothermal  
727 component in a metalliferous sediment core from the Mid-Atlantic Ridge. *Journal of*  
728 *Geophysical Research*, **98**, 9671-9681.  
729

730 Mills, R.A. & Elderfield, H. 1995. Hydrothermal activity and the geochemistry of  
731 metalliferous sediment. *Geophysical Monograph*, **91**, 392-407.  
732

733 Murphy, B.J., Waldron, J.W.F., Schofield, D.I., Barry, T.L. & Band, A. 2014. Highly  
734 depleted isotopic compositions evident in Iapetus and Rheic Ocean basalts: implications  
735 for crustal generation and preservation. *International Journal of Earth Sciences*, **103**,  
736 1219-1232.  
737

738 Nance, R.D., Murphy, J.B., Strachan, R.A., Keppie, J.D., Gutiérrez-Alonso, G.,  
739 Fernández-Suárez, J., Quesada, C., Linnemann, U., D'Lemos, R. & Pisarevsky, S.A.  
740 2008. Neoproterozoic - early Palaeozoic tectonostratigraphy and palaeogeography of the  
741 peri-Gondwanan terranes: Amazonian v. West African connections. *Geological Society*  
742 *of London*, **297**, 345-383.  
743

744 Pearce, J.A. 1996. A user's guide to basalt discrimination diagrams. *In: Wyman, D.A.*  
745 *(ed.) Trace element geochemistry of volcanic rocks: Applications for massive sulphide*  
746 *exploration*. Geological Association of Canada, 79-113.  
747

748 Peter, J.M. 2003. Ancient iron formations: their genesis and use in the exploration for  
749 stratiform base metal sulphide deposits, with examples from the Bathurst Mining Camp.  
750 *In: Lentz, D.R. (ed.) Geochemistry of Sediments and Sedimentary Rocks: Secular*  
751 *Evolutionary Considerations to Mineral Deposit-Forming Environments*. Geological  
752 Association of Canada, 145-176.  
753

754 Peter, J.M. & Goodfellow, W.D. 1996. Mineralogy, bulk and rare earth element  
755 geochemistry of massive sulphide-associated hydrothermal sediments of the Brunswick  
756 horizon, Bathurst mining camp, New Brunswick. *Canadian Journal of Earth Sciences*,  
757 **33**, 252-283.  
758

759 Piercey, S.J. 2007. Volcanogenic massive sulphide (VMS) deposits of the Newfoundland  
760 Appalachians: An overview of their setting, classification, grade-tonnage data, and  
761 unresolved questions. *In: Pereira, C.P.G. & Walsh, D.G. (eds.) Current Research*.  
762 Geological Survey Branch, St. John's, NL, 169-178.  
763

764 Piercey, S.J., Squires, G.C. & Brace, T.D. 2014. Lithostratigraphic, hydrothermal, and  
765 tectonic setting of the Boundary volcanogenic massive sulfide deposit, Newfoundland  
766 Appalachians, Canada: Formation by seafloor replacement in a Cambrian rifted arc.  
767 *Economic Geology*, **109**, 661-687, doi: 10.2113/econgeo.109.3.661.  
768

769 Pollock, J. 2004. Geology and Paleotectonic History of the Tally Pond Group, Dunnage  
770 Zone, Newfoundland Appalachians: An Integrated Geochemical, Geochronological,  
771 Metallogenic and Isotopic Study of a Cambrian Island Arc Along the Peri-Gondwanan  
772 Margin of Iapetus. M.Sc. Thesis, Memorial University of Newfoundland.  
773

774 Pollock, J.C. & Wilton, D.H.C. 2001. Metallogenic studies of the Tally Pond belt,  
775 Victoria Lake Group; trace-element geochemistry and lead-isotope data from the Exploits  
776 Subzone, Newfoundland. *Current Research Report 2001-1*, 247-266, Newfoundland and  
777 Labrador Department of Natural Resources, Geological Survey.  
778

779 Pollock, J.C., Wilton, D.H.C. & van Staal, C.R. 2002. Geological studies and definition  
780 of the Tally Pond Group, Victoria Lake Supergroup, Exploits Subzone, Newfoundland  
781 Appalachians. *Current Research Report 2002-1*, 155-167, Newfoundland and Labrador  
782 Department of Natural Resources, Geological Survey.  
783

784 Pollock, J.C., Hibbard, J.P. & van Staal, C.R. 2011. A paleogeographical review of the  
785 peri-Gondwanan realm of the Appalachian orogeny. This article is one of a series of  
786 papers published in this CJES Special Issue: In honour of Ward Neale on the theme of  
787 Appalachian and Grenvillian geology. *Canadian Journal of Earth Sciences*, 259-288, doi:  
788 10.1139/e11-049.  
789

790 Raczek, I., Jochum, K.P. & Hofmann, A.W. 2003. Neodymium and strontium isotope  
791 data for USGS reference materials BCR-1, BCR-2, BHVO-1, BHVO-2, AGV-1, AGV-2,  
792 GSP-1, GSP-2 and eight MPI-DING reference glasses. *The Journal of Geostandards and*  
793 *Geoanalysis*, **27**, 173-179.

794  
795 Rogers, N. 2004. Geochemical database, Red Indian Line project, central Newfoundland.  
796 *In: Canada, G.S.o. (ed.), Open File 4605.*

797  
798 Rogers, N., van Staal, C.R., McNicoll, V., Pollock, J., Zagorevski, A. & Whalen, J. 2006.  
799 Neoproterozoic and Cambrian arc magmatism along the eastern margin of the Victoria  
800 Lake Supergroup: A remnant of Ganderian basement in central Newfoundland?  
801 *Precambrian Research*, **147**, 320-341.

802  
803 Rogers, N., van Staal, C., Zagorevski, A., Skulski, T., Piercey, S.J. & McNicoll, V. 2007.  
804 Timing and tectonic setting of volcanogenic massive sulphide bearing terranes within the  
805 Central Mobile Belt of the Canadian Appalachians. *In: Milkereit, B. (ed.) Proceedings of*  
806 *Exploration 07: Fifth Decennial International Conference on Mineral Exploration*,  
807 Toronto, ON, 1199-1205.

808  
809 Rollinson, H.R. 1993. Using geochemical data: evaluation, presentation, interpretation.  
810 Longman, 352 p.

811  
812 Rudnicki, M.D. 1995. Particle formation, fallout and cycling within the buoyant and non-  
813 buoyant plume above the TAG vent field. *Geological Society, London, Special*  
814 *Publication*, **87**, 387-396, doi: 10.1144/gsl.sp.1995.087.01.30.

815  
816 Satkoski, A.M., Barr, S.M. & Samson, S.D. 2010. Provenance of Late Neoproterozoic  
817 and Cambrian sediments in Avalonia: Constraints from detrital zircon ages and Sm-Nd  
818 isotopic compositions in southern New Brunswick, Canada. *The Journal of Geology*, **118**,  
819 187-200.

820  
821 Schulz, K.J., Stewart, D.B., Tucker, R.D., Pollock, J.C. & Ayuso, R.A. 2008. The  
822 Ellsworth terrane, coastal Maine: Geochronology, geochemistry, and Nd-Pb isotopic  
823 composition--Implications for the rifting of Ganderia. *Geological Society of America*  
824 *Bulletin*, **120**, 1134-1158, doi: 10.1130/b26336.1.

825  
826 Spry, P.G., Peter, J.M. & Slack, J.F. 2000. Meta-exhalites as exploration guides to ore.  
827 *In: Spry, P.G., Marshall, B. & Vokes, F.M. (eds.) Metamorphosed and metamorphogenic*  
828 *ore deposits*. Society of Economic Geologists, Littleton, CO, 163-201.

829  
830 Squires, G.C. & Hinchey, J.G. 2006. *Geology of the Tally Pond Volcanic Belt and*  
831 *Adjacent Areas (parts of NTS 12A/09 & 12A/10). Map 2006-01.*

832  
833 Squires, G.C. & Moore, P.J. 2004. Volcanogenic massive sulphide environments of the  
834 Tally Pond Volcanics and adjacent area; geological, lithochemical and  
835 geochronological results. *In: Pereira, C.P.G., Walsh, D.G. & Kean, B.F. (eds.) Current*

836 *Research*. Geological Survey Branch, St. John's, NL, 63-91.  
837  
838 Sverjensky, D.A. 1984. Europium redox equilibria in aqueous solutions. *Earth and*  
839 *Planetary Science Letters*, **67**, 70-78.  
840  
841 Swinden, H.S. 1988. Introduction to volcanogenic sulphide deposits in Newfoundland.  
842 *In: Swinden, H.S. & Kean, B.F. (eds.) The volcanogenic sulphide districts of central*  
843 *Newfoundland*. Geological Association of Canada, 1-26.  
844  
845 \_\_\_\_\_ 1991. Paleotectonic settings of volcanogenic massive sulphide deposits in the  
846 Dunnage Zone, Newfoundland Appalachians. *Canadian Institute of Mining and*  
847 *Metallurgy Bulletin*, **84**, 59-89.  
848  
849 Swinden, H.S. & Thorpe, R.I. 1984. Variations in style of volcanism and massive sulfide  
850 deposition in Early to Middle Ordovician island-arc sequences of the Newfoundland  
851 Central Mobile Belt. *Economic Geology*, **79**, 1596-1619.  
852  
853 Tachikawa, K., Athias, V. & Jeandel, C. 2003. Neodymium budget in the modern ocean  
854 and paleo-oceanographic implications. *Journal of Geophysical Research*, **108(C8)**, 3254.  
855  
856 Tanaka, T., Togashi, S., Kamioka, H., Amakawa, H., Kagami, H., Hamamoto, T.,  
857 Yuhara, M., Orihashi, Y., Shigekazu, Y., Shimuzu, H., Kunimaru, T., Takahashi, K.,  
858 Yanagi, T., Nakano, T., Fujimaki, H., Shinjo, R., Asahara, Y., Tanimizu, M. &  
859 Dragusanu, C. 2000. JNdi-1: a neodymium isotopic reference in consistency with LaJolla  
860 neodymium. *Chemical Geology*, **168**, 279-281.  
861  
862 Tivey, M.K. 2007. Generation of seafloor hydrothermal vent fluids and associated  
863 mineral deposits *Oceanography*, **20**, 50-65.  
864  
865 Tosdal, R.M., Wooden, J.L. & Bouse, R.M. 1999. Pb isotopes, ore deposits, and  
866 metallogenic terranes. *Reviews in Economic Geology*, **12**, 1-28.  
867  
868 van Staal, C.R. & Barr, S.M. 2011. Lithospheric architecture and tectonic evolution of the  
869 Canadian Appalachians and associated Atlantic margin. *In: Percival, J.A., Cook, F.A. &*  
870 *Clowes, R.M. (eds.) Chapter 2 Tectonic Styles in Canada: the LITHOPROBE*  
871 *Perspective*. Geological Association of Canada, 3-55.  
872  
873 van Staal, C.R., Barr, S.M. & Murphy, J.B. 2012. Provenance and tectonic evolution of  
874 Ganderia: Constraints on the evolution of the Iapetus and Rheic oceans. *Geology*, **40**,  
875 987-990, doi: 10.1130/g33302.1.  
876  
877 Von Damm, K.L. 1990. Seafloor hydrothermal activity; black smoker chemistry and  
878 chimneys. *Annual Review of Earth and Planetary Sciences*, **18**, 173-204.  
879  
880 Williams, H. 1979. Appalachian Orogen in Canada. *Canadian Journal of Earth Sciences*,  
881 **16**, 792-807.

882  
883 Williams, H., Colman-Sadd, S.P. & Swinden, H.S. 1988. Tectonostratigraphic  
884 subdivisions of central Newfoundland. *Current Research, Part B*. Geological Survey of  
885 Canada, Ottawa, ON, Canada, 91-98.  
886  
887 Winchester, J.A. & Floyd, P.A. 1977. Geochemical discrimination of different magma  
888 series and their differentiation products using immobile elements. *Chemical Geology*, **20**,  
889 325-343.  
890  
891 Wood, S.A. & Williams-Jones, A.E. 1994. The aqueous geochemistry of rare-earth  
892 elements and yttrium. Part 4. Monazite solubility and REE mobility in exhalative massive  
893 sulfide-depositing environments. *Chemical Geology*, **115**, 135-162.  
894  
895 Zagorevski, A., van Staal, C.R., McNicoll, V.J. & Rogers, N. 2007. Upper Cambrian to  
896 Upper Ordovician peri-Gondwanan island arc activity in the Victoria Lake Supergroup,  
897 central Newfoundland; tectonic development of the northern Ganderian margin.  
898 *American Journal of Science*, **307**, 339-370.  
899  
900 Zagorevski, A., van Staal, C.R., Rogers, N., McNicoll, V.J. & Pollock, J. 2010. Middle  
901 Cambrian to Ordovician arc-backarc development on the leading edge of Ganderia,  
902 Newfoundland Appalachians. *Geological Society of America Memoir*, **206**, 367-396, doi:  
903 10.1130/2010.1206(16).  
904  
905  
906  
907  
908  
909  
910  
911  
912  
913  
914  
915  
916  
917  
918  
919  
920  
921  
922  
923  
924  
925  
926  
927

928 **Figure Captions**

929 **Fig. 1. (a)** Tectonostratigraphical assemblages with the main zones of the Newfoundland  
930 Appalachians (Avalon, Gander, Dunnage, and Humber zones) and VMS occurrences  
931 within the Notre Dame and Exploits subzones.

932 Notre Dame Subzone VMS: 1 – York Harbour; 2 – 8 - Baie Verte Belt Deposits; 9 – 12,  
933 46 – Springdale Belt Deposits; 13 – 29 Buchans-Roberts Arm Deposits.

934 Exploits Subzone VMS: 30 – 37 - Tulks Belt Deposits; Tally Pond Group Deposits: 39 –  
935 Lemarchant; 40 – Duck Pond; 41 – Boundary; 42 – 45 – Point Leamington Belt Deposits.

936 Modified after (Swinden, 1991) and Piercey (2007). **(b)** Geological map of the Tally  
937 Pond group. The Tally Pond group comprises the Lemarchant deposit and the Duck Pond  
938 and Boundary mines. Figure after Copeland (2009) and Map 2006-01 from Squires and  
939 Hinchey (2006) and Lode *et al.* (2017).

940

941 **Fig. 2. (a)** Fe-Ti/Al-Fe-Mn discrimination diagram indicating a hydrothermal origin for  
942 the Lemarchant exhalites. According to their higher Al-contents, tuff samples plot  
943 predominantly towards the right-hand side of the diagram, partially outside of the

944 hydrothermal field. Diagram after Boström (1973). **(b)** REE plus Y geospider plots of

945 Lemarchant proximal, distal, and interflow exhalites of various stratigraphical levels. All  
946 samples are normalized to the post-Archean Australian shale (PAAS) of McLennan  
947 (1989).

948

949 **Fig. 3.** Schematic illustration of the main aspects of hydrothermal circulation in  
950 extensional tectonic environments. In the recharge zone seawater is entrained through



951 crustal and progressively heated during downward migration. Water-rock interactions  
952 lead to loss of  $Mg^{2+}$ ,  $SO_4^{2-}$ , and  $OH^-$  and  $H_2S$  is generated. These reactions produce  $H^+$   
953 and create acidic fluids that leach metals out of rocks. In the reaction zone the highest  
954 temperatures are reached and the hydrothermal fluids gain their geochemical signatures.  
955 The hot fluids rise buoyantly up along synvolcanic faults and are expelled via the  
956 hydrothermal plume into the ambient seawater. Figure modified after German and Von  
957 Damm (2003) and Gibson *et al.* (2007).

958

959 **Fig. 4.** Core photographs of the main Lemarchant exhalite types and associated felsic and  
960 mafic volcanic rocks of the Bindons Pond and Lake Ambrose formations, respectively,  
961 and scanning electron microscope (SEM) image in back-scattered electron (BSE) mode  
962 of tuff intercalated with exhalite. **(a)** Finely laminated sulphide-rich EMS-type exhalite  
963 with cross-cutting stringer type veins and overlying massive sulphide mineralization.  
964 Section 101N, LM11-65, exhalite sample CNF30983, 160.7 m. **(b)** Proximal EMS-type  
965 exhalite associated with the Lemarchant Main Zone. Section 102+50N, LM10-43,  
966 CNF20976, 202.3 m. **(c)** Proximal EMS-type exhalite with intercalated chert-apatite  
967 layers. Section 101N, LM07-13, CNF30954, 164.7 m. **(d)** FEM-type exhalite associated  
968 with the Northwest Zone. Section 106N, LM08-28, CNF20986, 240.6 m. **(e)** Sulphide-  
969 rich interflow exhalite. Section 101+25N, LM13-79, CNF25072, 169.0 m. **(f)** Euhedral  
970 apatite (Ap) phenocrysts in an aphanitic quartz (Qz), feldspar, and chlorite-rich matrix of  
971 a vitric crystal tuff that is intercalated with FEM-type exhalite. Other phases are chlorite  
972 (Chl) in a vein, pyrite (Py), and barite (Brt). Section 104+51N, LM08-19, CNF30957a,  
973 98.89 m. **(g)** Felsic to intermediate volcanic rock of the Bindons Pond formation located

974 in the North target. Section 108N, LM11-49, 144.6 m. **(h)** Mafic to intermediate volcanic  
975 rock of the Lake Ambrose formation located in the North target. Section 108N, LM11-49,  
976 422.9 m.

977

978 **Fig. 5. (a)** Detailed photomicrograph (RL = reflected light). EMS-type exhalite, sample.  
979 with euhedral pyrite (Py), sphalerite (Sp) with chalcopyrite-disease, galena (Gn), and  
980 chalcopyrite (Ccp) S-isotopic spot analyses. Section 101+25N, LM13-79, CNF25071b,  
981 186.6 m. **(b)** Photomicrograph (RL) of framboid-rich EMS-type exhalite with a sulphide-  
982 rich vein parallel lamination. Vein sulphides consist of euhedral pyrite (Py), interstitial  
983 chalcopyrite (Ccp), and pyrrhotite (Po) and were analysed for S-isotopes. Section 105N,  
984 LM08-24ext, CNF20983, 432.8 m. **(c)**. Photomicrograph (RL) of a FEM-type exhalite,  
985 with euhedral and massive pyrite (Py), galena (Gn) inclusions, and associated interstitial  
986 chalcopyrite (Ccp) and S isotopic results of spot analyses. Section 103+25N, LM11-59,  
987 CNF30998, 194.2 m. **(d)**  $\delta^{34}\text{S}$  data ranges of pyrite (Py) including marcasite, pyrrhotite  
988 (Po), arsenopyrite (Apy), chalcopyrite (Ccp), and galena (Gn) with distribution shape and  
989 95<sup>th</sup> percentile (hatched line), as well as the average (solid line). Green bar on right-hand  
990 side indicates range of  $\delta^{34}\text{S}$  values that have only biogenically-derived S sources, based  
991 on two-component mixing modelling presented in Lode *et al.* (2017). Grey arrows  
992 display  $\delta^{34}\text{S}$  ranges that have mixed sources. Data are subdivided into the three exhalite  
993 types: EMS, FEM, and IFE. EMS-type exhalites have more contribution of S derived  
994 from thermochemical sulphate reduction than IFE-type exhalites. FEM-type show  
995 intermediate ranges.

996

997 **Fig. 6. (a)** Spatial distribution of  $\epsilon\text{Nd}$  for the EMS-, FEM-, and IFE-type exhalites and  
998 tuff, as well as the Lemarchant felsic and mafic volcanic rock from this study. Sample  
999 data do not show any spatial variations throughout the sections and/or with depth in the  
1000 stratigraphy in the Lemarchant area.  $2\sigma$  error bars calculated after algorithm from Ickert  
1001 (2013). **(b)** Resource map of the massive sulphides of the Lemarchant Main, 24 Zone,  
1002 and Northwest Zone. Massive sulphides are projected to the surface. Modified from the  
1003 resource map of Canadian Zinc Corporation.

1004

1005 **Fig. 7. (a)** Diagram of  $\epsilon\text{Nd}$  versus Th/Sc ratio for the three main types of Lemarchant  
1006 exhalites (EMS, FEM, and IFE) and tuff. Also plotted are data from Rogers *et al.* (2006)  
1007 for felsic and mafic volcanic rocks of the Tally Pond group and the Crippleback/Sandy  
1008 Brook Group crustal basement rocks. Mid Ocean Ridge Basalt (MORB) field from data  
1009 from Gale *et al.* (2014). Arc andesite field from data from Hawkeswoth *et al.* (1979). All  
1010 data re-calculated for  $\epsilon\text{Nd}_{513}$ . Diagram modified after McLennan *et al.* (1993). **(b)** Plot of  
1011  $f^{\text{Sm/Nd}}$  versus  $\epsilon\text{Nd}$  for the EMS-, FEM-, and IFE-type exhalites and tuff, as well as the  
1012 Lemarchant felsic and mafic volcanic rock from this study. Also plotted are data from  
1013 Rogers (2004) and Rogers *et al.* (2006) for felsic and mafic volcanic rocks of the Tally  
1014 Pond group, a felsic volcanic rock samples from the unmineralized Upper Block at Duck  
1015 Pond and a sample from the Mineralized Block at Duck Pond from data from McNicoll *et*  
1016 *al.* (2010), and the Crippleback/Sandy Brook Group crustal basement rocks. Diagram  
1017 modified after McLennan *et al.* (1993).

1018

1019 **Fig. 8.** Zr/Ti versus Nb/Y plot for volcanic rocks after Winchester and Floyd (1977) and  
1020 Pearce (1996) for the Lemarchant felsic and mafic volcanic rocks from this study and  
1021 from data from Rogers (2004) and Rogers *et al.* (2006). Additionally, data fields for  
1022 felsic, intermediate, and mafic volcanic rocks was added (Cloutier *et al.*, 2017). Data  
1023 from Rogers (2004) and Rogers *et al.* (2006) was also used to plot the Crippleback  
1024 Lake/Sandy Brook Group crustal basement rocks.

1025

1026 **Fig. 9.** Model displaying the Cambrian Tally Pond group with juvenile Nd signatures that  
1027 is built upon the Ganderian and Gondwanan Amazonian rifted crustal basement with  
1028 evolved Nd signatures. **(a)** Early stages of arc rifting with felsic volcanism and formation  
1029 of massive sulphides and genetically associated exhalites. Scavenged and detrital juvenile  
1030 and evolved Nd is archived in the exhalites resulting in mixed signatures. **(b)** Final stages  
1031 of arc rifting and emplacement of mafic volcanic rocks that form the hanging wall to the  
1032 Lemarchant VMS deposit.

1033

1034 **Fig. 10.** Diagram of  $\epsilon_{Nd}$  versus age for Tally Pond group exhalite and volcanic rock  
1035 samples from this study and from Rogers (2004), Rogers *et al.* (2006), and McNicoll *et*  
1036 *al.* (2010). The field for Ganderian Neoproterozoic rocks is from Rogers *et al.* (2006).  
1037 Fields for the Mesoproterozoic Amazonian crust, the Transamazonian crust, and the West  
1038 African Craton are from Satkoski *et al.* (2010) and references therein. Depleted mantle  
1039 evolution curve is from dePaolo (1981). CHUR = Chondrite uniform reservoir.

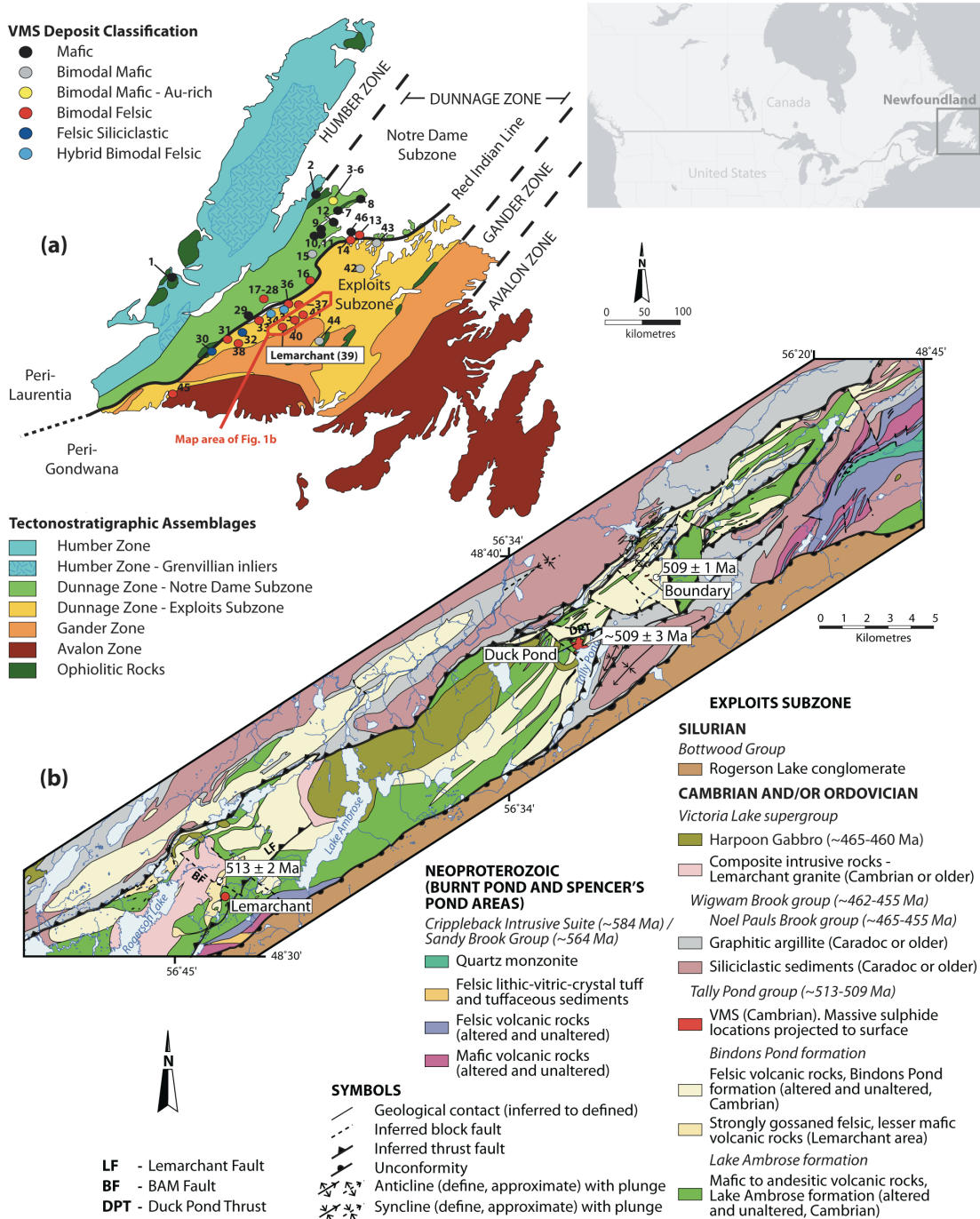
1040

1041

1042

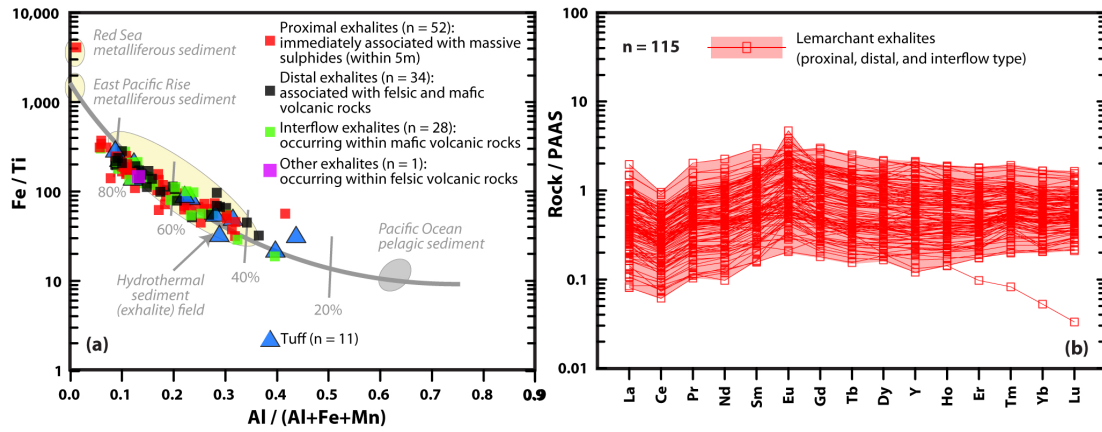
1043

Lode, Stefanie Fig. 1



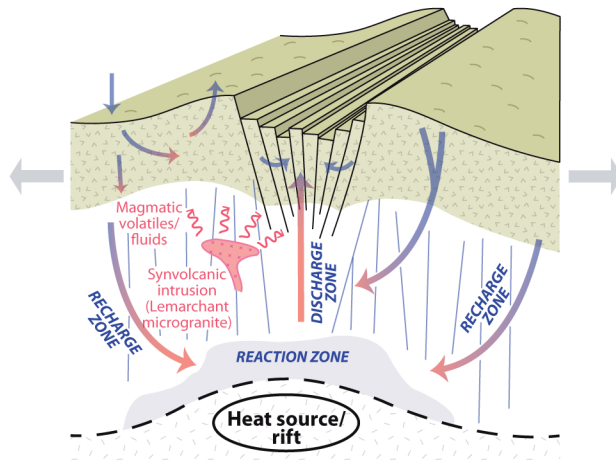
1044  
1045

Lode, Stefanie Fig. 2



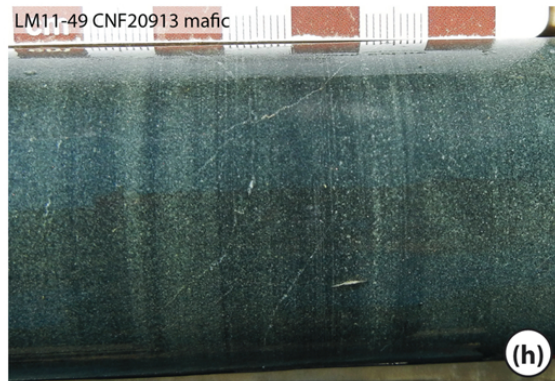
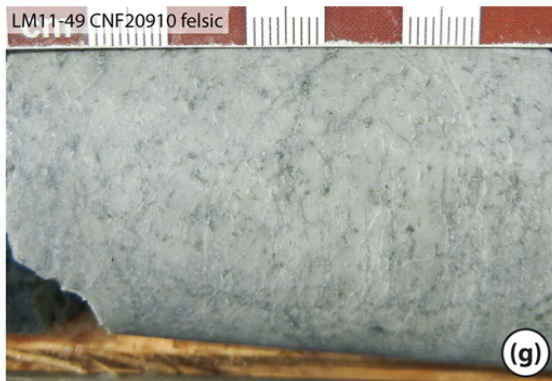
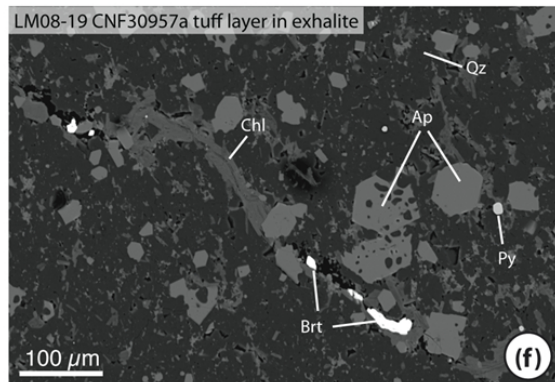
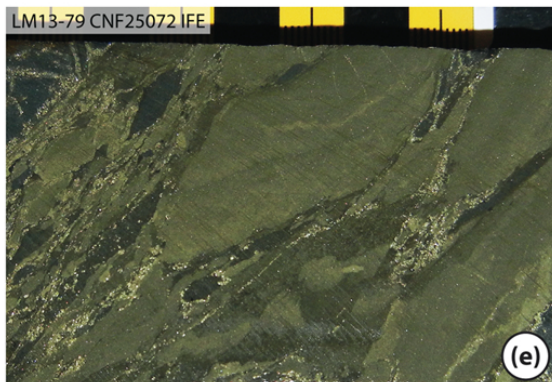
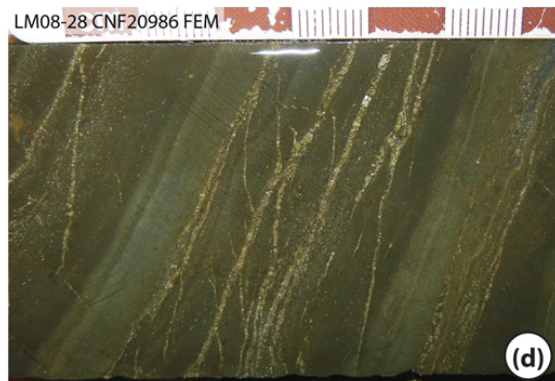
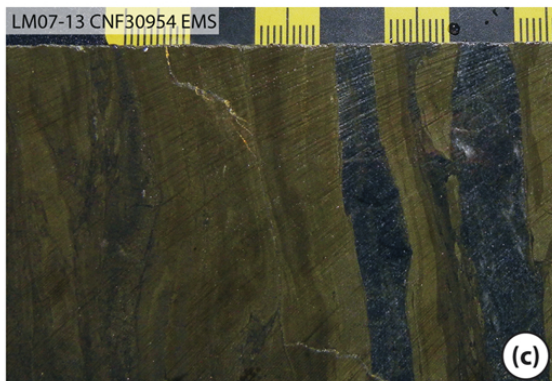
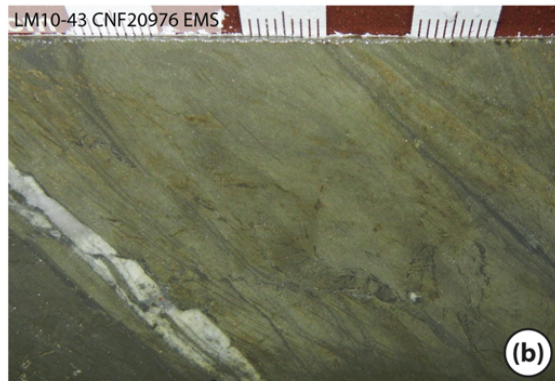
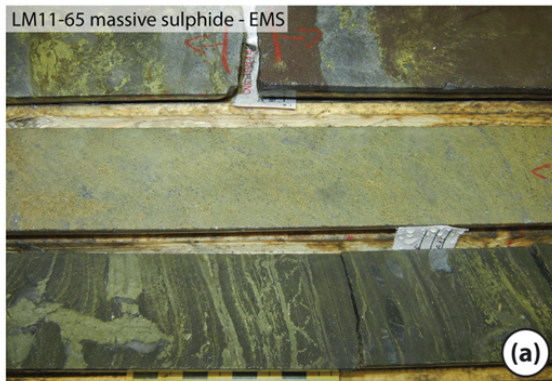
1046  
1047

Lode, Stefanie Fig. 3



1048  
1049

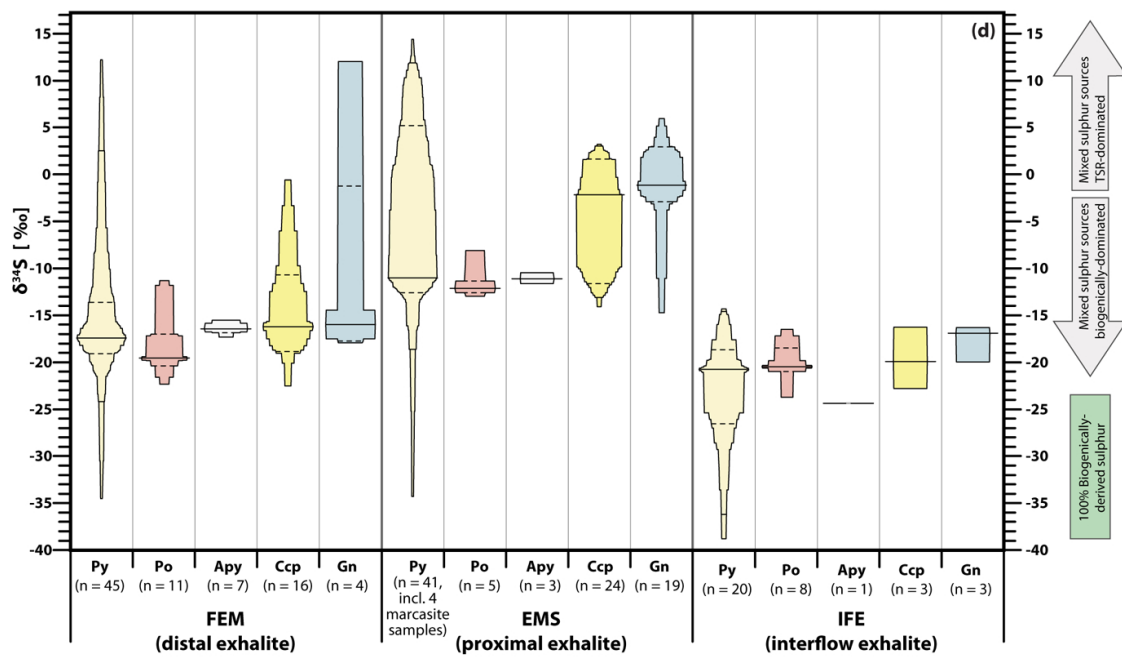
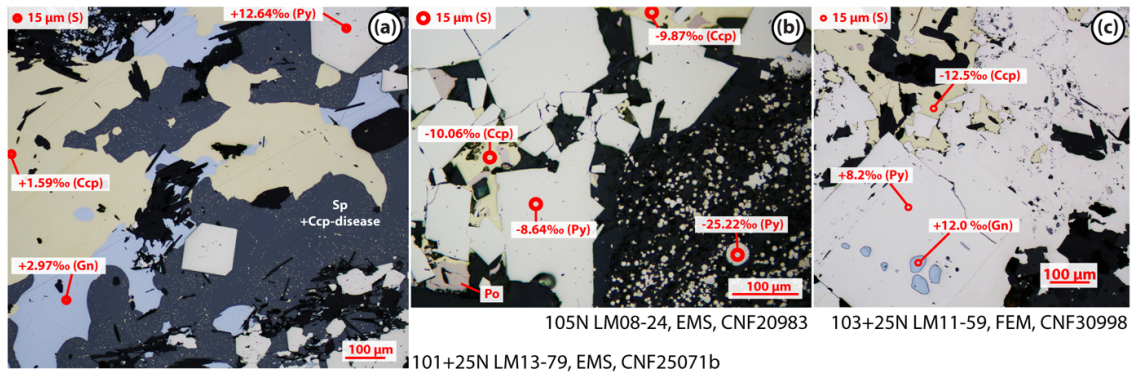
Lode, Stefanie Fig. 4



1050  
1051

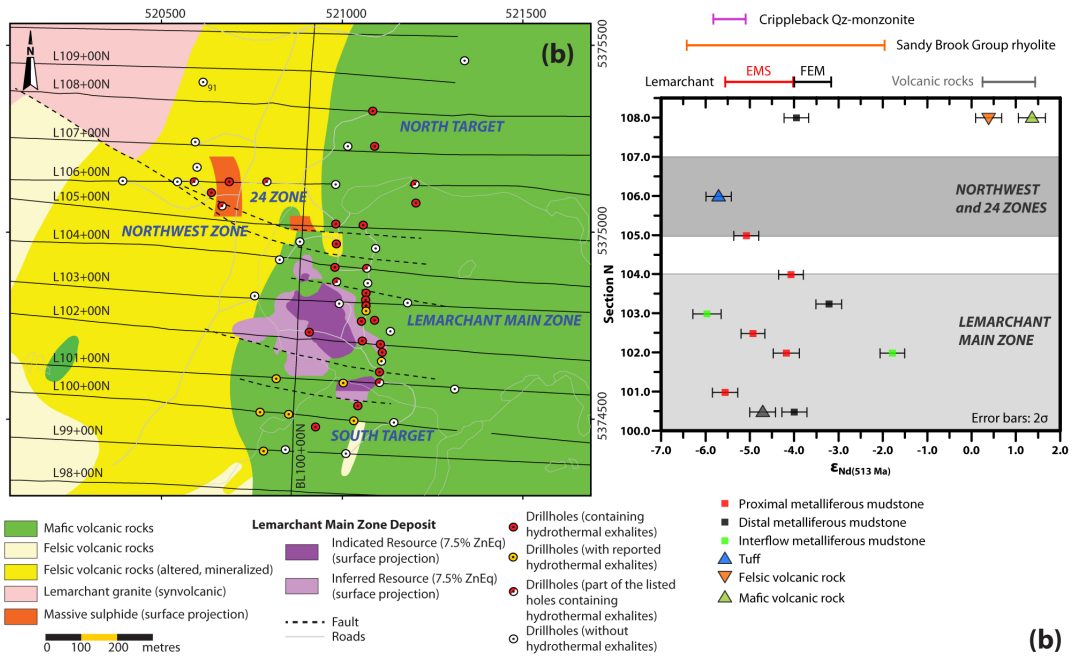


Lode, Stefanie Fig. 5



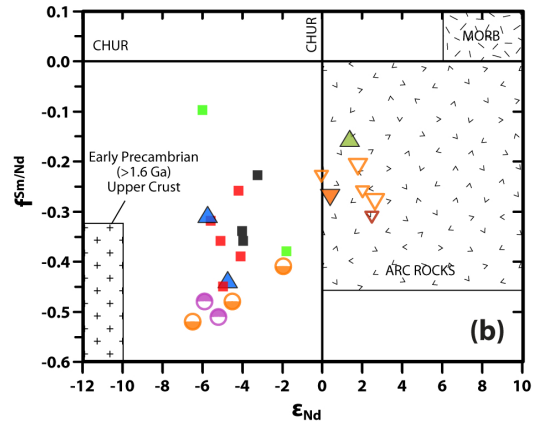
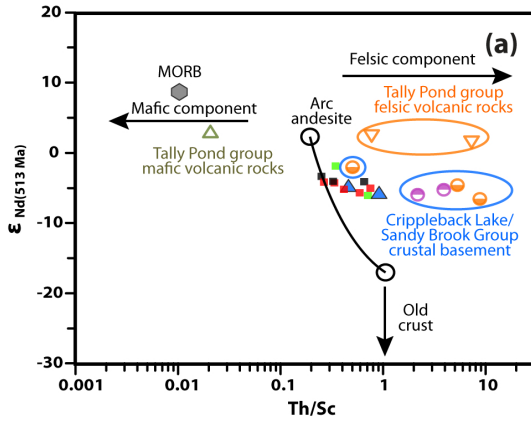
1052  
1053

Lode, Stefanie Fig. 6



1054  
1055

Lode, Stefanie Fig. 7



Data from this study ( $\epsilon_{Nd_{513}}$ )

- Lemarchant proximal mudstone
- Lemarchant distal mudstone
- Lemarchant interflow mudstone
- ▲ Lemarchant tuff
- ▼ Lemarchant felsic to intermediate volcanic rock,
- ▲ Lemarchant mafic to intermediate volcanic rock, Lemarchant

Data from Rogers (2004) and Rogers et al. (2006)

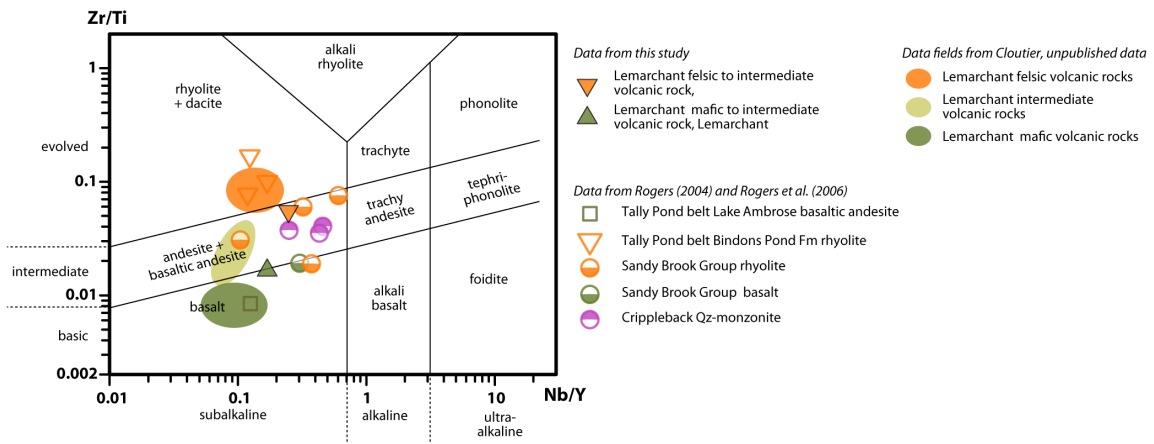
- ▲ Tally Pond belt Lake Ambrose basalt ( $\epsilon_{Nd_{513}}$ )
- ▼ Tally Pond belt Bindons Pond Fm rhyolite ( $\epsilon_{Nd_{513}}$ )
- Sandy Brook Group rhyolite ( $\epsilon_{Nd}$ )
- Crippleback Qz-monzonite ( $\epsilon_{Nd}$ )

Data from McNicoll et al. (2010)

- ▼ Duck Pond Upper Block rhyolite and dacite ( $\epsilon_{Nd_{513}}$ )
- ▼ Duck Pond Mineralized Block ore horizon (felsic volcanic rocks) ( $\epsilon_{Nd_{509}}$ )

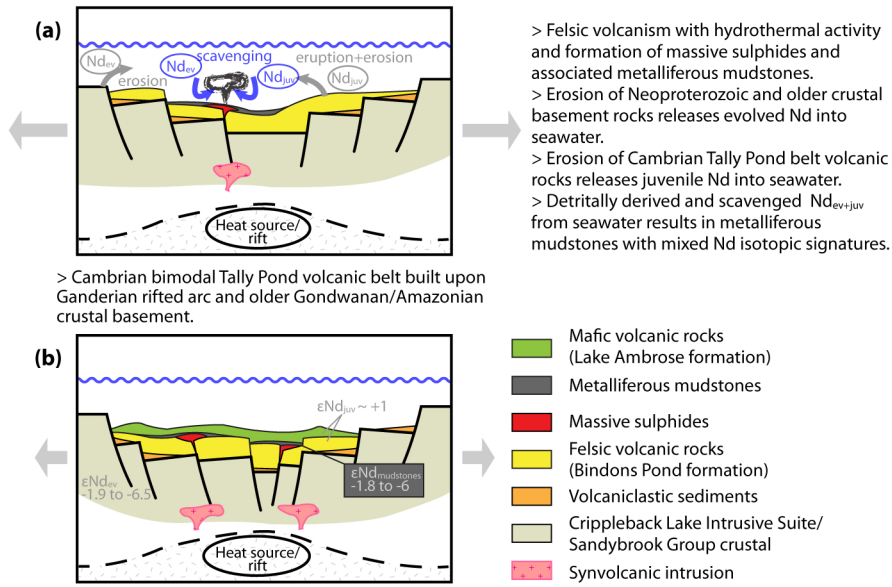
1056  
1057

Lode, Stefanie Fig. 8



1058  
1059

Lode, Stefanie Fig. 9



1060  
1061

Lode, Stefanie Fig. 10

